Received: 18 November 2016 | Revised: 24 April 2017 | Accepted: 25 April 2017

DOI: 10.1002/jnr.24083

RESEARCH ARTICLE

WILEY

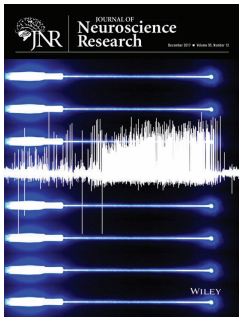

Leukemia/lymphoma-related factor (LRF) exhibits stage- and context-dependent transcriptional controls in the oligodendrocyte lineage and modulates remyelination

Nathan L. Davidson[1] | Fengshan Yu[2] | Naruchorn Kijpaisalratana[3] | Tuan Q. Le[2] | Laurel A. Beer[2] | Kryslaine L. Radomski[2] | Regina C. Armstrong[1,2]

[1]Program in Neuroscience, Bethesda, Maryland, USA

[2]Department of Anatomy, Physiology, and Genetics, Uniformed Services University of the Health Sciences, Bethesda, Maryland, USA

[3]Department of Internal Medicine, Faculty of Medicine, Chulalongkorn University, Bangkok, Thailand

Correspondence
Regina C. Armstrong, Department of Anatomy, Physiology, and Genetics, Uniformed Services University of the Health Sciences, 4301 Jones Bridge Rd., Bethesda, MD, 20814.
Email: regina.armstrong@usuhs.edu

Funding information
The National Multiple Sclerosis Society, grant/award number: RG 4224; RG 4675.

Abstract

Leukemia/lymphoma-related factor (LRF), a zinc-finger transcription factor encoded by *Zbtb7a*, is a protooncogene that regulates differentiation in diverse cell lineages, and in the CNS, its function is relatively unexplored. This study is the first to examine the role of LRF in CNS pathology. We first examined LRF expression in a murine viral model of spinal cord demyelination with clinically relevant lesion characteristics. LRF was rarely expressed in oligodendrocyte progenitors (OP) yet, was detected in nuclei of the majority of oligodendrocytes in healthy adult CNS and during remyelination. *Plp/CreER^T:Zbtb7a$^{fl/fl}$* mice were then used with cuprizone demyelination to determine the effect of LRF knockdown on oligodendrocyte repopulation and remyelination. Cuprizone was given for 6 weeks to demyelinate the corpus callosum. Tamoxifen was administered at 4, 5, or 6 weeks after the start of cuprizone. Tamoxifen-induced knockdown of LRF impaired remyelination during 3 or 6-week recovery periods after cuprizone. LRF knockdown earlier within the oligodendrocyte lineage using *NG2CreER^T:Zbtb7a$^{fl/fl}$* mice reduced myelination after 6 weeks of cuprizone. LRF knockdown from either the *Plp/CreER^T* line or the *NG2CreER^T* line did not significantly change OP or oligodendrocyte populations. *In vitro* promoter assays demonstrated the potential for LRF to regulate transcription of myelin-related genes and the notch target Hes5, which has been implicated in control of myelin formation and repair. In summary, in the oligodendrocyte lineage, LRF is expressed mainly in oligodendrocytes but is not required for oligodendrocyte repopulation of demyelinated lesions. Furthermore, LRF can modulate the extent of remyelination, potentially by contributing to interactions regulating transcription.

KEYWORDS
demyelination, cuprizone, notch, differentiation, oligodendrocyte progenitor

1 | INTRODUCTION

Therapeutic strategies for multiple sclerosis aim to attenuate the autoimmune response, prevent axon degeneration, and facilitate recovery of function through remyelination. Promoting the differentiation of oligodendrocyte progenitor (OP) cells is an area of intense interest as a means to enhance remyelination (Kremer, Kury, & Dutta, 2015).

Nathan L. Davidson and Fengshan Yu contributed equally to this work.

Significance

Regulation of oligodendrocyte progenitor (OP) differentiation and oligodendrocyte myelination is critical for effective remyelination and recovery of function in multiple sclerosis and other demyelinating diseases. We previously showed that leukemia/lymphoma-related factor (LRF) promotes OP differentiation during postnatal myelination. We now examine LRF during CNS remyelination. We show that LRF is rarely detected in OP cells yet is present in nuclei of the majority of oligodendrocytes in healthy and remyelinating CNS. In vitro, LRF regulates transcription of myelin-related genes and notch target genes. In vivo, LRF is not required for oligodendroglial repopulation of demyelinated lesions yet modulates remyelination.

Differentiation within the oligodendrocyte lineage is regulated by complex mechanisms that work together to accomplish derepression of myelin genes (Liu & Casaccia 2010). Many components involved in these processes have been identified but the molecular interactions are not yet fully understood. Moreover, mechanisms may be modulated in different contexts, such as developmental myelination, myelin remodeling in normal adults, or remyelination in adult pathology.

In the environment of demyelinated lesions, reactive astrocytes and activated microglia/macrophages express molecular signals that act, through transcriptional controls, to regulate OP differentiation (Gallo & Deneen, 2014). Multiple transcription factors that regulate OP differentiation can interact with histone deacetylase 1 (HDAC1), including leukemia/lymphoma-related factor (LRF), myelin transcription factor 1, and Yin-Yang1 (Armstrong, Kim, & Hudson, 1995; Dobson, Moore, Tobin, & Armstrong, 2012; He, Sandoval, & Casaccia-Bonnefil, 2007; Liu et al., 2004; Nielsen, Berndt, Hudson, & Armstrong, 2004; Romm, Nielsen, Kim, & Hudson, 2005). Each of these potential transcriptional repressors exhibits stage-specific expression within the oligodendrocyte lineage. In addition, HDAC1 represses the transcription factor Hes5 to promote OP differentiation and mediate derepression of myelin genes (Liu et al., 2006; Shen et al., 2008).

The notch-signaling pathway is one of the potent inhibitors of OP differentiation that limit remyelination (Hammond et al., 2014; Zhang et al., 2009). Jagged1, a notch ligand, is expressed in hypertrophic astrocytes in active multiple sclerosis plaques lacking remyelination (John et al., 2002). Notch1 acts through Hes5 to inhibit OP differentiation (Wu, Liu, Levine, & Rao, 2003). Hes5 is progressively down-regulated during OP differentiation yet elevated in demyelinated lesions in which remyelination is limited, such as in chronic lesions of multiple sclerosis (John et al., 2002; Kondo & Raff, 2000; Liu et al., 2006; Wang et al., 1998).

LRF warrants particular interest as a potential point of intersection between HDAC1 promoter regulation and notch signaling. LRF has been referred to as the "most exciting yet enigmatic" member of the POK/ZBTB family of transcription factors, which generally act as transcriptional repressors (Lunardi, Guarnerio, Wang, Maeda, & Pandolfi, 2013). The 43 known members of this protein family contain a POK/BTB domain at the N terminus, which mediates protein-protein interactions, while the C terminus contains multiple Kruppel-type zinc fingers that bind DNA. The gene zinc finger and BTB domain-containing protein 7A (Zbtb7a) encodes the protein referred to as LRF (mouse), OCZF (rat), or FBI-1 (human) and will be referred to as LRF here. LRF binds corepressors and recruits HDAC1 to gene targets with consensus LRF binding sites (Liu et al., 2004; Lunardi, Guarnerio, Wang, Maeda, & Pandolfi, 2013). LRF plays a critical role in promoting differentiation of B cells by suppressing Notch1 signals that instruct differentiation along the T cell lineage (Lee et al., 2013; Maeda et al., 2007). In multiple cell lines, LRF also interacts with sterol regulatory element-binding protein (SREBP) to synergistically activate transcription of fatty acid synthase (FASN), which is essential for phospholipids in myelin and cell membranes (Choi et al., 2008). In OP cells, SREBPs are important regulators of oligodendrocyte maturation and FASN levels (Monnerie et al., 2017). However, LRF activity can be stage-specific as shown for transcriptional regulation in the osteoclast lineage and also for fetal to adult type globin gene expression in erythroid cells (Masuda et al., 2016; Tsuji-Takechi et al., 2012). Indeed, among hematopoietic lineages, LRF regulates differentiation by complexing with different key factors in a tissue- and context-dependent manner (Lunardi et al., 2013).

In the brain and spinal cord, LRF is strongly expressed in the nuclei of oligodendrocytes as well as in diverse neuronal populations (Dobson, Moore, Tobin, & Armstrong, 2012). LRF expression in these postmitotic neural cells in the normal postnatal and adult CNS contrasts with the pro-mitotic role of LRF in cancer (Lee & Maeda, 2012). LRF expression co-localized with NeuN in nuclei of both large motor neurons in the ventral horn and small sensory dorsal horn neurons, as well as in multiple neuronal populations distinguished by their size and laminar distribution in the cerebral cortex (Dobson et al., 2012). In white matter of the postnatal spinal cord, LRF was expressed in only about 10% of OP cells in contrast to over 70% expression of LRF in oligodendrocytes (Dobson et al., 2012). Regardless of lineage stage, LRF was localized in nuclei. In vitro, viral transduction of LRF promoted OP differentiation, while LRF knockdown impaired OP differentiation (Dobson et al., 2012). Furthermore, in vivo deletion of LRF inhibited OP differentiation and the generation of mature oligodendrocytes during postnatal myelination (Dobson et al., 2012).

The present study characterizes the expression and role of LRF in OP cells and mature oligodendrocytes during remyelination. Given the context-dependent activity of LRF noted above in other cell types, we characterize LRF expression using a murine hepatitis virus (MHV) model to produce focal demyelinating lesions in the spinal cord with gliosis, inflammation, and breakdown of the blood-brain barrier that reflects the complex pathology of multiple sclerosis lesions (Armstrong, Redwine, & Messersmith, 2005; Messersmith, Murtie, Le, Frost, & Armstrong, 2000; Redwine & Armstrong, 1998; Vana, Lucchinetti, Le, & Armstrong, 2007b). We cross floxed *Zbtb7a* mice with *Plp/CreER*^{T} and *NG2CreER*^{T} lines for tamoxifen-induced conditional deletion of LRF in oligodendrocyte lineage cells following cuprizone demyelination. We have previously used this system with the cuprizone model to identify molecular interactions contributing to effective remyelination (Zhou, Pannu, Le, & Armstrong, 2012). In vitro promoter assays demonstrate the potential for LRF to

regulate transcription of myelin genes and notch target genes during OP differentiation. Our studies demonstrate that LRF expression in the oligodendrocyte lineage is mainly found in oligodendrocytes during remyelination and that LRF can modulate the extent of remyelination.

2 | MATERIALS AND METHODS

Animals were housed and handled according to the guidelines of the National Institutes of Health and the Institutional Animal Care and Use Committee of the Uniformed Services University of the Health Sciences.

2.1 | MHV model of spinal cord demyelination and remyelination in *C57BL/6* mice

C57BL/6 mice (4-week old females; Jackson Laboratories) were infected with 1000 plaque forming units (PFU) of MHV strain A59 diluted in 10 μL of sterile PBS by intracranial injection as previously described (Armstrong et al., 2005; Redwine & Armstrong 1998; Vana et al., 2007b). Control mice were injected with 10 μL of sterile PBS. Only female mice were used because males have a high mortality rate after infection with this MHV A59 strain (Armstrong et al., 2005). Behavioral data was previously published for this cohort of mice and demonstrated neurological impairment (hang times and paralysis/paresis) of MHV-infected mice by 2 weeks post-infection (wpi) prior to random assignment to either a 4- or 8-wpi survival time point (Redwine & Armstrong, 1998). Spinal cord tissue analysis included a cohort of 12 mice (MHV 4 wpi, $n = 3$; MHV 8 wpi, $n = 3$; PBS vehicle 4 wpi, $n = 3$; PBS 8 wpi, $n = 3$).

2.2 | Cuprizone model of demyelination and remyelination in *Zbtb7a*$^{fl/fl}$ mice

Initial heterozygous breeding pairs of the floxed *Zbtb7a* mouse line were provided by Dr. Pier Paola Pandolfi (Beth Israel Deaconess Medical Center; Maeda et al., 2007). Floxed *Zbtb7a* mice were crossed to *Plp/CreER*^{T} mice, in which the proteolipid (Plp) promoter drives conditional oligodendrocyte expression of Cre recombinase fused to a mutated estrogen receptor. Breeding pairs of *Plp/CreER*^{T} mice (B6.Cg-Tg[Plp1-cre/ERT]3Pop/J; Doerflinger, Macklin, & Popko, 2003) and *NG2CreER*^{T} mice (B6.Cg-Tg[Cspg4-cre/Esr1*]BAkik/J; Zhu et al., 2011) were purchased from Jackson Laboratories. Mice were genotyped by PCR analysis of tail genomic DNA to identify wild type and floxed alleles of *Zbtb7a* and the presence or absence of the *Cre* allele (Doerflinger et al., 2003; Maeda et al., 2007).

Cuprizone, also known as bis(cyclohexanone)oxaldihydrazone, was purchased as a fine powder (Sigma-Aldrich) that was sent to Harlan Teklad to mix as 0.2% or 0.3% (w/v) to form chow pellets (diet TD.01453; Harlan Teklad). Male mice were fed cuprizone pellets for a period of 6 weeks followed by 0, 3, or 6 weeks on normal chow. Since cuprizone causes toxicity resulting in estrus cycle disruption in female C57BL/6 mice, male mice were used (Taylor, Gilmore, Ting, & Matsushima, 2010). At the start of cuprizone feeding, mice were 8 weeks of age and weighed 22.88 ± 1.14 g (s.d.). To accommodate the pre-cuprizone wheel testing, mice in the wheel running cohorts were between 10-14 weeks of age and weighed 25.54 ± 1.46 g (s.d.) at the start of cuprizone feeding. To maximize demyelination and further differentiate effects on oligodendrocyte repopulation during remyelination, mice were fed 0.2% cuprizone in the initial wheel running cohort and then 0.3% cuprizone for the subsequent wheel running cohort.

To induce Cre-mediated deletion of *Zbtb7a*, 10 mg of tamoxifen (Sigma-Aldrich) in corn oil (Sigma-Aldrich) was administered by oral gavage after 4, 5, or 6 weeks of cuprizone demyelination (as noted in the text) or in age-matched control mice. Control mice received oral gavage with the corn oil vehicle in parallel with the mice who were administered tamoxifen. The Cre deletion of *Zbtb7a* analysis used 65 mice, which, as noted in figure legends, included 5-7 mice per condition and time point. Sample size was based on prior data and the feasibility of breeding matched cohorts of mice to run together in a given experiment. Mice were randomly assigned to tamoxifen or corn oil conditions.

2.3 | Immunohistochemistry and in situ hybridization

Mice were perfused with 4% paraformaldehyde (Sigma-Aldrich) and post-fixed in 4% paraformaldehyde overnight at 4 °C. Segments of brain or spinal cord were cut as cryosections (15 μm thickness) and mounted onto Superfrost Plus slides (Fisher) for immunohistochemical analysis and in situ hybridization.

Antibody information is provided in Table 1. Tissue sections were immunostained for LRF using two different antibodies, which have been characterized in our previous developmental study (Dobson et al., 2012). LRF immunolabeling was further tested to ensure specificity in lesion areas of MHV spinal cord sections. LRF immunostaining produced a similar pattern of nuclear immunofluorescence with the two different primary antibodies, and was eliminated with either omission of the primary antibody or incubation of the primary antibody with a 100 × excess of competitive blocking peptide (Bethyl Laboratories; Supplemental Figure S1). Oligodendrocyte lineage cells were identified by expression of Olig2. OP cells were immunolabeled with an antibody to the external domain of NG2 (Goretzki, Burg, Grako, & Stallcup, 1999; Jones, Yamaguchi, Stallcup, & Tuszynski, 2002). Oligodendrocytes were identified by antibodies against glutathione S-transferase pi (GSTpi) or adenomatous polyposis coli. Myelin was immunostained for 2',3'-cyclic-nucleotide 3'-phosphodiesterase (CNP) or myelin oligodendrocyte glycoprotein (MOG; Breithaupt et al., 2003; Linnington, Webb, & Woodhams, 1984). Organization of the node of Ranvier was detected by immunolabeling Nav1.6 sodium channels in the node along with contact in associated protein (Caspr) in the flanking paranodal regions. The LRF primary antibodies were detected with goat anti-hamster IgG F(ab')2 fragment conjugated with Cy3, or donkey anti-rabbit IgG F(ab')2 fragment conjugated with Cy3 (both from Jackson Immunoresearch). Donkey anti mouse IgG F(ab')2 fragment conjugated with Cy3 (Jackson Immunoresearch) was used to detect MOG. Olig2, NG2, GSTpi, CNP, and Hes5 were detected by goat anti-rabbit or donkey anti-rabbit IgG F(ab')2 fragment conjugated with Alexa Fluor 488 (Invitrogen, Carlsbad,

TABLE 1 Primary antibodies used

Used to Detect	Antibody	Species	Dilution	Source	Immunogen	Cat# (RRID)
LRF	LRF 13E9	Hamster monoclonal	1:100	Santa Cruz Biotechnology; Santa Cruz, CA	Human residues 1-20	sc-33683 (AB 668999)
LRF	Zbtb7a/FBI-1	Rabbit polyclonal	1:10,000	Bethyl Laboratories; Montgomery, TX	Human residues 200 and 250	A300-548A (AB 2273107)
Oligodendrocyte lineage cells	Olig2	Rabbit polyclonal	1:100	Millipore; Billerica, MA	Mouse Olig-2	AB15328 (AB 2299035)
Oligodendrocyte progenitors	NG2 extracellular domain	Rabbit polyclonal	1:500	Dr. William Stallcup, Burnham Institute; La Jolla, CA	Rat residues 1-2223	(AB 2572306)
Oligodendrocytes	Glutathione S-transferase pi (GSTpi)	Rabbit polyclonal	1:500	MBL International; Nagoya, Japan	Human GSTpi	311 (AB 212153)
Oligodendrocytes	Adenomatous polyposis coli (CC1)	Mouse monoclonal	1:200	Millipore; Billerica, MA	Human residues 1-226	444904 (AB 212153)
Myelin	2',3'-cyclic-nucleotide 3'-phosphodiesterase (CNP)	Mouse monoclonal	1:100	Cell Signaling Technology; Danvers, MA	Human CNPase residues surrounding Val81	2986S (AB 2082474)
Myelin	Myelin oligodendrocyte glycoprotein (MOG) 8-18C5	Mouse monoclonal	1:20	Dr. Christopher Linington, University of Glasgow; Glasgow, UK	Rat cerebellar glycoproteins (8-18C5 binds to MOG residues 101-108)	(AB 2631445)
Caspr	Paranodal region	Mouse monoclonal K65/35	1:500	NeuroMab; Davis, CA	Cytoplasmic domain (1308-1381 of rat Caspr)	75-001 (AB_2083496)
Nav1.6	Node of Ranvier	Rabbit polyclonal	1:100	Alomone Labs; Jerusalem, Israel	Intracellular loop between domains II and III (residues 1042-1061 of rat Nav1.6)	ASC-009 (AB_2040202)

CA). Donkey anti-rabbit IgG F(ab)2 fragment conjugated to Alexa Fluor 594 was used to detect Nav1.6 while Caspr was detected by donkey anti-mouse IgG F(ab')2 fragment conjugated to Alexa Fluor 488 (both from Jackson Immunoresearch). Protocols were optimized to ensure that no signal was observed when primary antibody was not applied. All sections were incubated with DAPI (Sigma-Aldrich) to stain nuclei prior to mounting with Vectashield (Vector Labs).

In situ hybridization was performed using a previously described riboprobe to hybridize to PLP mRNA transcripts as a marker of oligodendrocytes (Armstrong, Le, Frost, Borke, & Vana, 2002). After hybridization, labeling was detected with alkaline phosphatase-conjugated sheep anti-digoxigenin, followed by reaction with substrate solution (nitroblue tetrazolium chloride/5-bromo-4-chloro-3-indolylphosphate [NBT/BCIP]; DAKO).

2.4 | OP enriched cultures and transient transfection

As detailed previously, OP cultures were prepared and grown in defined medium to induce differentiation or with mitogens added to inhibit differentiation (Armstrong, 1998; Zhou & Armstrong, 2007). Briefly, brains from P2 rats were dissociated and plated in tissue culture flasks to produce stratified "primary" cultures. After shaking to dislodge microglia, flasks were shaken overnight to yield OP cells. Preliminary studies were performed using the previously characterized CNP promoter construct (Nielsen et al., 2004) to optimize the number of cells to plate per well, the ratio of transfection reagents, and the time point for luciferase analysis (data not shown). The same protocol was then followed for all subsequent experiments. Cells were plated at a concentration of 120,000 cells per well in 24-well plates in defined medium, supplemented with platelet-derived growth factor-AA (PDGF) and fibroblast growth factor 2 (FGF2; both 10 ng/ml; R&D Systems) to induce proliferation and prevent differentiation. One day after plating, the cells were transiently transfected by incubation for 5 hours with plasmid constructs and a 9:1 ratio of FuGENE®6 (Promega). The cultures were maintained for 1 day in defined medium (with PDGF and FGF2), and then transferred to defined medium (either with or without PDGF and FGF2) for one more day. Cells were then lysed and harvested for luciferase analysis at a total of 72 hours, post-plating, to examine promoter activity relative to continued OP proliferation or during OP differentiation.

2.5 | Promoter reporter assays

The LRF-expressing plasmid (Lenti-TomLRF) contains full length murine *Zbtb7a*, followed by an IRES sequence, and a tdTomato fluorescent reporter (pLVX-IRES-tdTomato; Clontech); the pLVX-IRES-tdTomato

backbone without the LRF insert was used as a reference control (Dobson et al., 2012). The OP cultures were additionally transfected with one of several firefly-luciferase reporter plasmids, each driven by a unique promoter sequence. Plasmids with firefly-luciferase expression, controlled by the promoters for *Hes1* (pHes1; −467 to + 46) and *Hes5* (pHes5; −800 to + 73) were used to study the response of these Notch targets (kind gifts from Dr. Ryoichiro Kageyama, Kyoto University; Ohtsuka et al., 1999). Transfection with the Notch1 intracellular domain (Notch1IC; kind gift from Dr. Nye, Pharmacia) inserted into the PMX vector was used to increase the level of expression of both Hes1 and Hes5 (Nye, Kopan, & Axel, 1994; Zhou & Armstrong, 2007). The CNP reporter is driven by 3.7kb of the CNP promoter (Nielsen et al., 2004). The 1323MBP reporter uses the −1323 to + 30 region of the myelin basic protein (*MBP*) gene to drive firefly expression, while 105MBPwt uses only the −105 to + 30 region of *MBP*. The 105MBPmut plasmid contains a mutation in the GC box sequence of the 105MBPwt plasmid, where CCG has been mutated to TGA (each kind gifts from Robin Miskimins, University of South Dakota; Wei, Miskimins, & Miskimins, 2003). The plasmid for fatty acid synthase, which is encoded by the *FASN* gene, contains the full-length FASN promoter driving firefly luciferase (kind gift from Timothy F. Osborne, University of California, Irvine; Choi et al., 2008; Jeon et al., 2008). Two additional plasmids were used as reference controls across experiments: a plasmid with CMV-driven expression of eGFP and firefly luciferase was used as a positive control (pEGFPLuc; Clontech), while a truncated version of this plasmid (0GFP) with the CMV promoter region excised by the NheI and AseI restriction enzymes was used as a negative control (Nielsen et al., 2004).

Transfection ratio of plasmids was established as 150 ng of the Lenti-TomLRF plasmid or the pLVX-IRES-tdTomato control, 150 ng of the luciferase reporter plasmid, and 20 ng of the pRL-SV40 Renilla luciferin reporter internal control (Promega). In the case of Hes1 and Hes5, 150 ng of either the Notch1IC-PMXs or the PMXs control plasmid was also added. The Dual-Luciferase® Reporter assay system (Promega) was used to quantify the luciferase response on the Synergy™ H1 Multi-Mode Reader (Bio-Tek).

2.6 | Imaging, quantification, and statistical analysis

All images were acquired with a Spot 2 digital camera mounted to an IX-70 microscope (Olympus), with the exception of the node of Ranvier, which was imaged as fluorescent image stacks acquired using a Zeiss LSM 700 (Carl Zeiss Microscopy). Figures were prepared as panels using Adobe Photoshop (RRID: SCR_014199). In transverse spinal cord sections, quantification areas were delimited as white matter areas with demyelination identified by MOG or CNP immunostaining and matched to the same anatomical area in the control mice. In the coronal sections of corpus callosum, the myelinated area was estimated from MOG immunolabeling, as previously detailed (Armstrong, Le, Flint, Vana, & Zhou, 2006). MetaMorph Image Analysis Software (RRID: SCR_002368; Molecular Devices) was used to threshold pixels as above baseline for positive myelin staining within the section. Within each area of spinal cord or corpus callosum, all labeled cells were counted manually with a 40x objective lens. Spot Advanced Software (RRID: SCR_014313; Spot Imaging Solutions) was used to measure the area of each region-of-interest. As noted in the figure legends, three sections per mouse were analyzed for three or more mice in each condition, and quantifications were performed blinded to the condition. By dividing the firefly reading by the reading of the *Renilla* control for each OP culture experiment, three biological-replicate samples from each condition were collected and normalized and four independent experiments were combined by calculating the weighted mean and variance for each condition.

GraphPad Prism 7.01 (RRID: SCR_002798; Graphpad) was used for statistical calculations and graphing. Unpaired Student's *t*-test was used to compare two conditions at a single time point, with the Kolmogorov-Smirnov test to confirm normality and Cohen's *d* calculation of the effect size. Analysis of variance was used to compare across multiple time points and/or conditions. One-way analysis of variance was followed by a Tukey post-hoc adjustment for multiple comparisons. Fisher's combined *t*-test and Stouffer's Z-score were used to corroborate the validity of these combined results. To analyze in vitro assays with two growth conditions for each of two combinations of plasmids, two-way analysis of variance was used and followed by Holm-Sidak's adjustment for multiple comparisons. For clarity, only statistically significant differences are noted. A p-value $< .05$ was considered statistically significant.

3 | RESULTS

3.1 | LRF expression in oligodendrocyte lineage cells during demyelination and remyelination

We first asked whether LRF was differentially expressed in the oligodendrocyte lineage during the progression of demyelinating disease with spontaneous remyelination. MHV infection results in oligodendrocyte loss over 2-3 wpi that causes focal demyelination throughout the spinal cord followed by OP amplification by 4 wpi, which then advances to oligodendrogenesis and remyelination by 8 wpi (Redwine & Armstrong, 1998; Vana et al., 2007b). Immunohistochemistry for LRF, along with CNP to detect myelin, demonstrates the pattern of LRF expression relative to demyelination. Normal myelination is observed in PBS-injected control mice (Figure 1a) with LRF expressed in the nuclei of smaller cells throughout the white matter as well as in relatively large gray matter neurons (Figure 1a). The majority of oligodendrocyte lineage cells, detected by Olig2, exhibit nuclear LRF in normal white matter (PBS controls; Figure 1a,d,g). At 4 wpi, focal demyelination is evident based on the loss of immunoreactivity for myelin proteins, MOG (data not shown), or CNP (Figure 1b), as well as by loss of Olig2 cells (Figure 1e,g). Specifically, the population of Olig2 cells that express LRF is significantly reduced (Figure 1g). LRF cells without Olig2, i.e. non-oligodendrocyte lineage cells, are abundant in demyelinated lesions and co-label for markers of lymphocytes, microglia, and astrocytes (Supplemental Figure S2). At 8 wpi, demyelination is no longer detected using CNP immunostaining (Figure 1c) and lesion areas are repopulated by Olig2 cells (Figure 1f,g). The total Olig2 population,

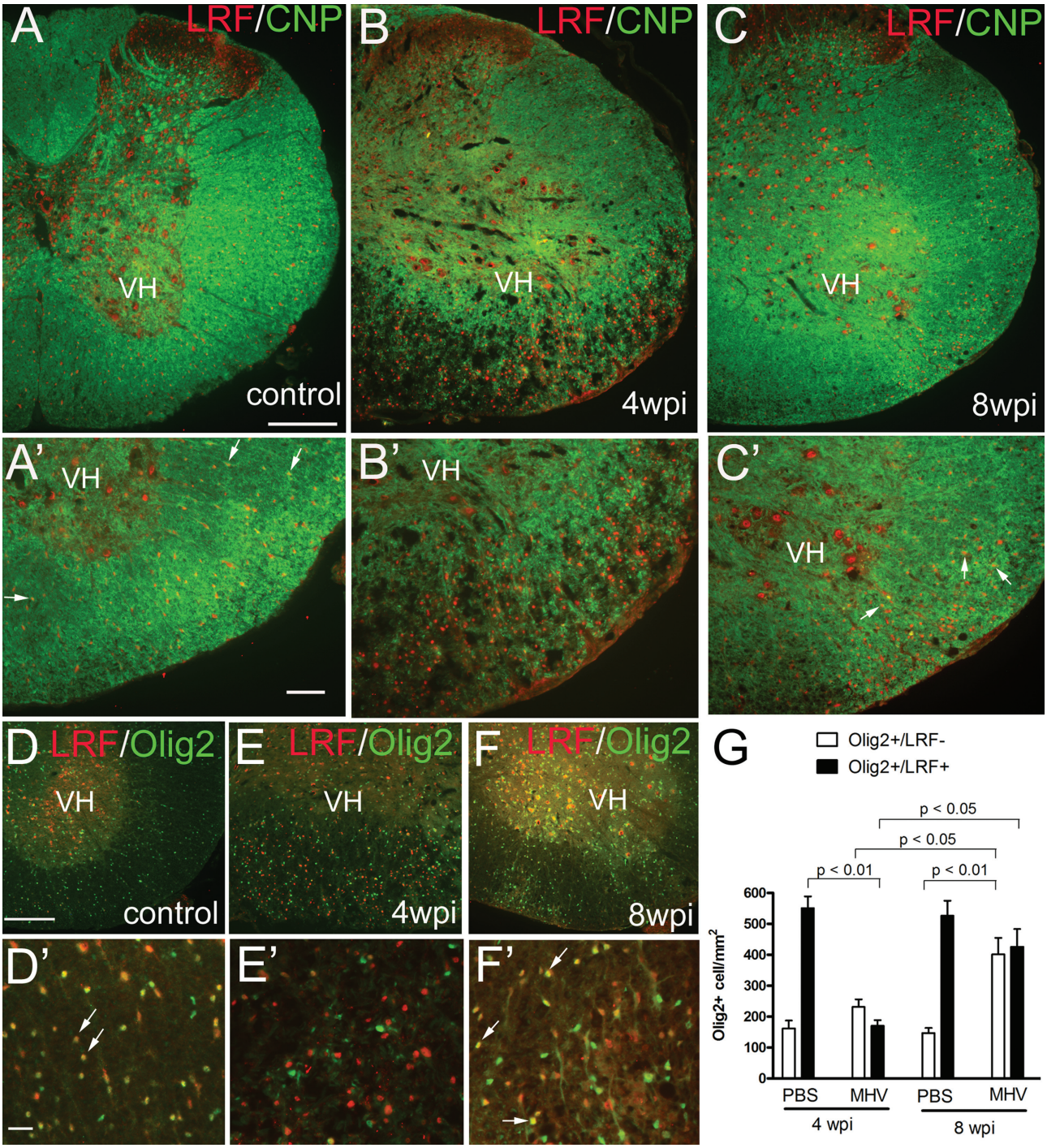

FIGURE 1 Oligodendrocyte lineage expression of LRF during the progression of demyelination and remyelination. Spinal cord transverse sections immunostained for LRF (red) in combination with CNP (A-C'; green) or Olig2 (D-G; green). In control white matter (A, D; PBS-injected match to 4 wpi MHV), LRF is present in the nuclei of oligodendrocytes labeled by CNP (arrows in A') or by Olig2 (arrows in D'). The majority of Olig2 cells express LRF in control white matter (G). During demyelination (4 wpi; B, B'), lesion areas have a loss of CNP immunoreactivity and reduction of Olig2 cells in white matter (G). In demyelinated lesions, a high density of LRF + cells are not labeled with CNP (B') or Olig2 (E'), indicating infiltration of non-oligodendrocyte lineage cells. As remyelination progresses, CNP immunolabeling shows myelin throughout the white matter although mild vacuolization and cellular infiltrate are still visible adjacent to the ventral root exit zone, a typical lesion site (8 wpi; C, C'). Many cells immunolabeled for CNP (arrows in C') or Olig2 (arrows in F') exhibit nuclear LRF at 8 wpi. Olig2 cell populations recover by 8 wpi and the distribution of Olig2 cells is almost evenly split among those with or without LRF (G). Olig2 nuclear immunoreactivity was used to identify oligodendrocytes, as was clearly visible even at lower magnifications (D-F). A low intensity of Olig2 immunoreactivity in processes was detectable in lesion areas at higher magnifications (E', F'), which was considered non-specific signal due to changes in the lesion tissue. One way ANOVA using $n = 3$ mice for each condition; $p = 0.0022$, F (3,8) = 12.46 for Olig2 + LRF- cells; $p = 0.0009$, F (3,8) = 16.29 for Olig2 + LRF + cells. Scale bars A-C, D-F = 200 um, A'-C' – 75 um, D'-F' = 25 um. VH = spinal cord ventral horn.

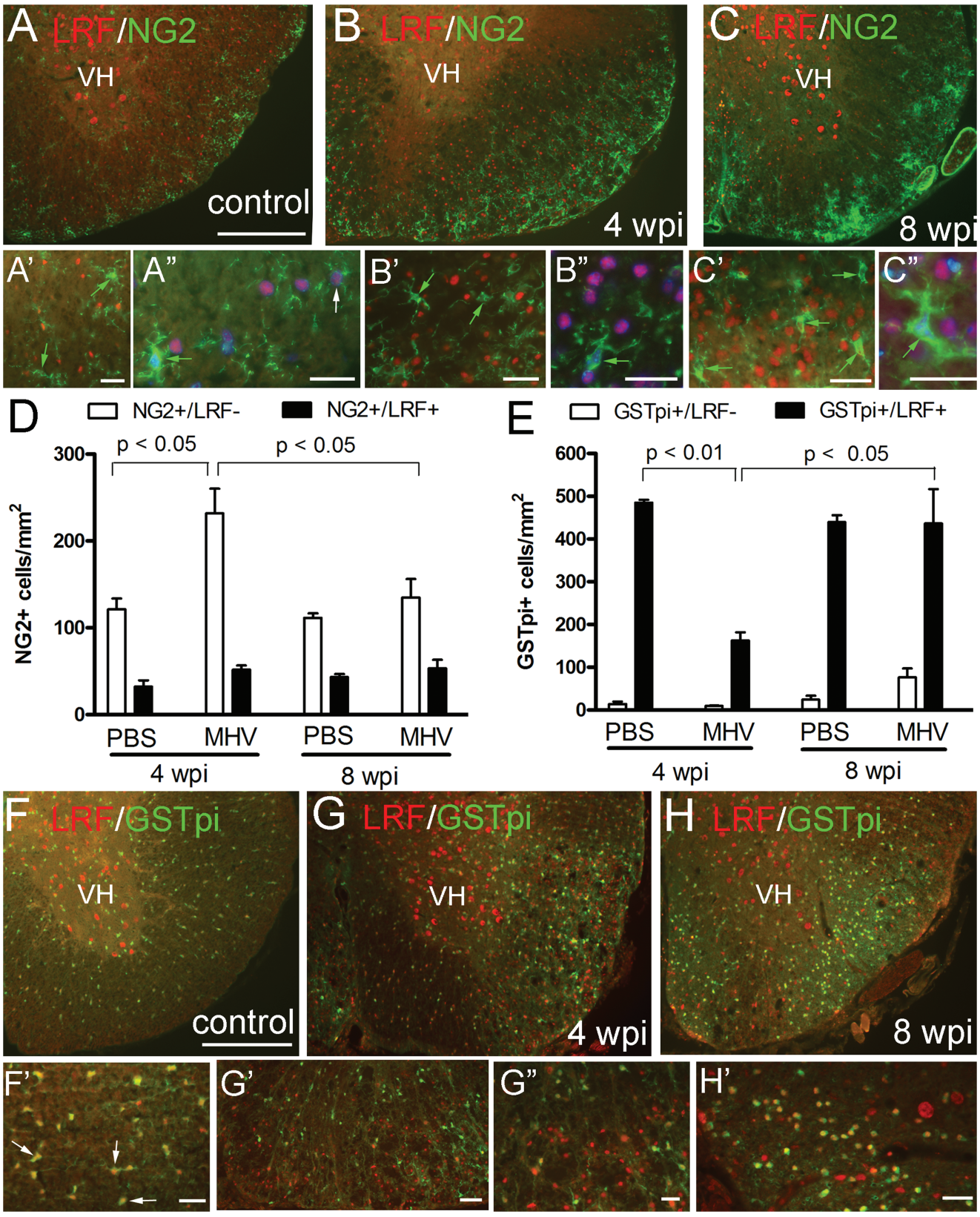

FIGURE 2.

with and without LRF expression, shows recovery of the oligodendrocyte lineage cells from approximately 400 cells/mm^2 at 4 wpi to over 800 cells/mm^2 at 8 wpi (Figure 1g).

LRF expression in specific stages of oligodendrocyte lineage cells was distinguished by immunolabeling for NG2 to detect OP cells (Figure 2a-d) and for GSTpi to detect mature oligodendrocytes (Figure

2e-h). In non-lesioned adult white matter, the majority of NG2 cells do not express LRF (see PBS controls in Figure 2a,d). The NG2 population is increased in demyelinated lesions (Figure 2b,d). The amplified NG2 population mainly does not express LRF (Figure 2d). In contrast, GSTpi labeled oligodendrocytes are significantly reduced in demyelinated lesions (Figure 2e), and comprise over a 66% reduction of GSTpi labeled cells expressing LRF in demyelinated lesions (Figure 2e,g). During remyelination, GSTpi cells recover to control levels (Figure 2e,h). However, in MHV mice at 8 wpi the population of cells that expressed Olig2 without LRF is approximately 400 cells/mm^2 (Figure 1g), which is larger than the approximately 200 cells/mm^2 from the combination of NG2 and GSTpi cells without LRF (Figure 2d,e). Therefore, the LRF negative population includes a stage of cells detected by Olig2 and not accounted for by NG2 or GSTpi. Overall, LRF expression corresponds strongly with mature oligodendrocytes and changes along with the oligodendrocyte population throughout the progression from demyelination to remyelination.

3.2 | Conditional inducible knockdown of LRF during remyelination in *Plp/CreER^T:Zbtb7a$^{fl/fl}$* mice

Our results show that oligodendrocytes are the main lineage stage expressing LRF in normal adult white matter and after MHV infection. Therefore, we used *Plp/CreER^T:Zbtb7a$^{fl/fl}$* mice for tamoxifen-induced genetic inactivation of LRF in vivo to test the effect of LRF loss in oligodendrocytes during remyelination. The corpus callosum was demyelinated by feeding mice 0.2% cuprizone for 6 weeks. Tamoxifen, or oil as the vehicle control, was administered at the end of cuprizone ingestion to knockdown the LRF expression and examine the effect on spontaneous remyelination during the subsequent 6-week period on normal chow.

Effective LRF knockdown was demonstrated in *Plp/CreER^T:Zbtb7a$^{fl/fl}$* by double labeling nuclei for LRF and Olig2, a marker of oligodendrocyte lineage cells (Figure 3a-b). Tamoxifen administration significantly reduced expression of LRF among Olig2 immunolabeled cells (Figure 3c-f). This effective LRF knockdown did not change the overall density of Olig2 cells (Figure 3g). Since the mice used to demonstrate LRF knockdown had a 6 week recovery period to allow for remyelination, effective demyelination at 6 weeks of cuprizone in *Plp/CreER^T:Zbtb7a$^{fl/fl}$* mice could not be confirmed in those same mice. Therefore, additional mice fed 0.2% cuprizone along with the LRF knockdown cohort were perfused at the end of the 6-week period of cuprizone feeding to confirm corpus callosum demyelination (Figure S3).

The cohort of mice with demonstrated LRF knockdown was then analyzed to determine the extent of remyelination after the 6-week recovery period. MOG immunostaining showed remyelination had progressed in mice administered either oil (Figure 4a) or tamoxifen (Figure 4b) while quantification showed a significant reduction in the tamoxifen condition (Figure 4c). The MOG area reduction is modest but the tamoxifen area values are below the 97th percentile of the oil area values, based on a large Cohen's *d* effect size. However, the density of oligodendrocytes identified by PLP expression was not different between mice administered tamoxifen versus oil (Figure 4d-f). Furthermore, LRF knockdown did not alter the populations within the oligodendrocyte lineage identified as OP cells by NG2 expression (Figure 4g-i) or as mature oligodendrocytes by CC1 immunoreactivity (Figure 4j-l).

Longitudinal analysis of behavior was included in the study design to assess the behavioral effect of LRF knockdown during the subsequent remyelination period (Figure S4). Running activity on wheels with a complex pattern of rungs was used to detect impaired maximal running velocity, which is associated with myelination status of the corpus callosum in longitudinal studies of mice fed cuprizone (Hibbits, Pannu, Wu, & Armstrong, 2009; Mierzwa, Zhou, Hibbits, Vana, & Armstrong, 2013). In the current study, mice had wheels continuously available for running and every third week the wheel was changed from a training wheel (all rungs in place) to a complex wheel (non-uniform pattern of missing rungs). The same *Plp/CreER^T:Zbtb7a$^{fl/fl}$* mice that are shown for tissue analysis in Figures 3, 4 had running wheel data collected. These mice exhibited impaired maximal running velocity during cuprizone feeding, consistent with demyelination (Figure S4a). However, during the recovery period, there was no functional effect of LRF knockdown, based on comparison of mice administered tamoxifen versus oil (Figure S4a).

The effect of the 6-week 0.2% cuprizone treatment on maximal running velocity was significant, but not as marked as in our prior studies (Hibbits et al., 2009; Mierzwa et al., 2013), which may be due to the

FIGURE 2 Stage-specific expression of LRF in the oligodendrocyte lineage during the progression of demyelination and remyelination. Spinal cord transverse sections immunostained for LRF (red) in combination with NG2 (green) to identify oligodendrocyte progenitor cells (A-D) or GSTpi (green) to identify oligodendrocytes (E-H'). **A-D**: In the control white matter (A-A"; PBS-injected match to 4 wpi MHV), LRF is typically absent from NG2 cells (examples shown with green arrows) but was found in the nucleus of some NG2 cells, particularly NG2 cells with rounded nuclei (example at white arrow). In response to demyelination, there is a significant increase in the density of NG2 cells without LRF in white matter of MHV infected mice (4 wpi; B, with quantification in D). As remyelination progresses, NG2 cell density normalizes (8 wpi; C, D). NG2 cells with thickened processes indicative of a reactive phenotype remain in lesion areas at 8 wpi (C"). At both 4 and 8 wpi, lesion areas contain many LRF cells that do not express NG2 (B', C'). **E-H**: In control white matter (F; PBS-injected match to 4 wpi MHV), LRF is expressed in the vast majority of cells immunolabeled for GSTpi (white arrows in F'). During demyelination, there is a significant reduction in the density of GSTpi cells expressing LRF (4 wpi; E, G, G', G"). As remyelination progresses, GSTpi cell density normalizes (8 wpi; E, H, H'). The proportion of GSTpi cells expressing LRF is similar between normal and remyelinating white matter (8 wpi; E). DAPI nuclear stain shown in blue. One way ANOVA using $n = 3$ mice for each condition; $p = 0.0071$, $F(3,8) = 8.536$ for NG2 + LRF-, $p = 0.1816$, $F(3,8) = 2.078$ for NG2 + LRF+, $p = 0.0133$, $F(3,8) = 6.87$ for GSTpi + LRF-, $p = 0.0024$, $F(3,8) = 12.15$ for GSTpi + LRF+. Scale bars = 200 μm (A-C, F-H), 25 μm (all subset images). VH = spinal cord ventral horn.

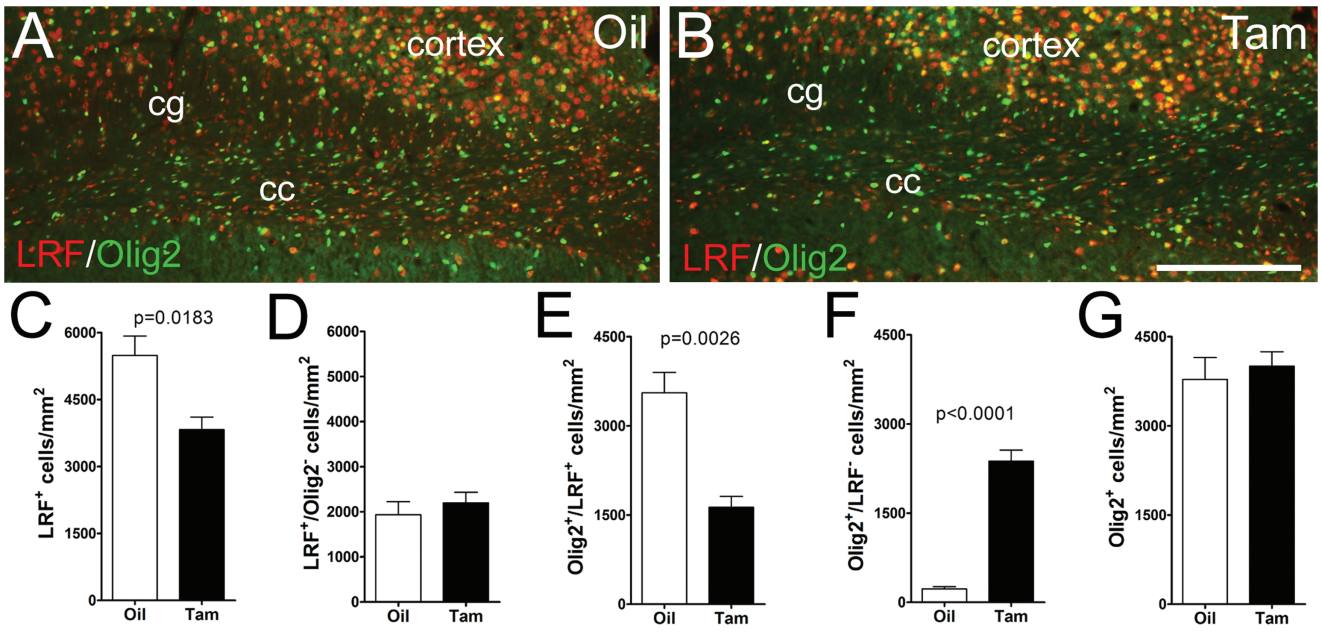

FIGURE 3 Knockdown of LRF in oligodendrocytes during remyelination. Demyelination of the corpus callosum was induced in *Plp/CreERT:Zbtb7a*$^{fl/fl}$ mice by feeding 0.2% cuprizone for 6 weeks. Mice were then administered tamoxifen (Tam), or vehicle (Oil), followed by 6 weeks on a normal chow diet to allow for spontaneous remyelination. **A-B**: Coronal brain sections immunolabeled for Olig2 (green) to identify oligodendrocyte lineage cells and quantify expression of LRF (red) in mice administered vehicle (A) or tamoxifen (B). LRF is present in cells of the white matter including the corpus callosum (cc) and overlying cingulum (cg) and is strongly expressed in neurons, such as those of the adjacent cortex. **C-G**: Quantification of LRF and Olig2 labeling in the corpus callosum. LRF is significantly reduced in mice administered tamoxifen (C). Confirming appropriate conditional expression from the *Plp/CreERT* line, this LRF reduction is restricted to the oligodendrocyte lineage since cells that are not labeled for Olig2 do not show reduced LRF (D). Among cells expressing Olig2, those double labeled for LRF are significantly reduced in mice administered tamoxifen (E). Mice administered oil have few Olig2 cells that are not labeled with LRF (F). The total population of Olig2 cells is unchanged by tamoxifen administration and reduction of LRF expression (G). Scale bar = 250 um. Student *t*-test using $n = 4$ mice in each condition.

continuous availability of the wheels in the current study. A subsequent cohort of *Plp/CreER*^{T}*:Zbtb7a*$^{fl/fl}$ mice was treated with 0.3% cuprizone (Figure S4b). The higher cuprizone dose was used to maximize demyelination and oligodendrocyte loss while maintaining continuous availability of wheels to maintain the same paradigm used for the 0.2% cuprizone cohort. The results with 0.3% cuprizone again showed there was no difference between mice administered tamoxifen versus oil during the recovery period.

Tamoxifen was next administered at earlier time points after cuprizone in *Plp/CreER*^{T}*:Zbtb7a*$^{fl/fl}$ mice to further test the effect of LRF knockdown at an earlier stage of oligodendrocyte regeneration and remyelination. Tamoxifen was administered after week 5, and cuprizone ingestion was again used at the 0.3% dose to maximize demyelination and for tissue analysis along with the 0.3% cuprizone cohort that was tested on the wheel assay. At 6 weeks of cuprizone, mice were either perfused or given a 3-week recovery period on normal chow for analysis of early remyelination. Mice examined at the end of the 6 weeks of 0.3% cuprizone showed effective demyelination (Figure 5a). During the subsequent 3-week recovery period, remyelination was significantly reduced in mice administered tamoxifen (Figure 5b). While the MOG area reduction is modest, the tamoxifen area values are below the 90th percentile of the oil area values, based on a large Cohen's *d* effect size. Using the mice from the complex wheel behavioral assessment, oligodendrogenesis and remyelination were also examined with tamoxifen administered at 6 weeks of 0.3% cuprizone, followed by 6 weeks for recovery on normal chow. Again, mice administered tamoxifen exhibited significantly less remyelination after the 6-week recovery period (Figure 5c). The MOG area reduction is modest yet the tamoxifen area values are below the 95th percentile of the oil area values, based on a large Cohen's *d* effect size calculation. In addition, the node of Ranvier organization is disrupted during cuprizone demyelination and continues to be markedly disorganized at 3 weeks after ending cuprizone (data not shown). With the progression of remyelination at 6 weeks after cuprizone, immunolabeling for Caspr and Nav1.6 shows relatively normal nodal structure in mice administered oil while examples of disrupted broader nodes continued to be found in mice administered tamoxifen (Figure 5c). Tamoxifen administration did not alter the density of oligodendrocytes at any of the time points (Figure 5d-f). These results with 0.3% cuprizone show that LRF knockdown reduces the extent of remyelination but does not alter oligodendrocyte repopulation of the corpus callosum. Therefore, LRF knockdown produced a relatively modest but significant reduction in remyelination in 3 independent cohorts of mice after either 0.2% (Figure 4c) or 0.3% cuprizone (Figure 5b,c).

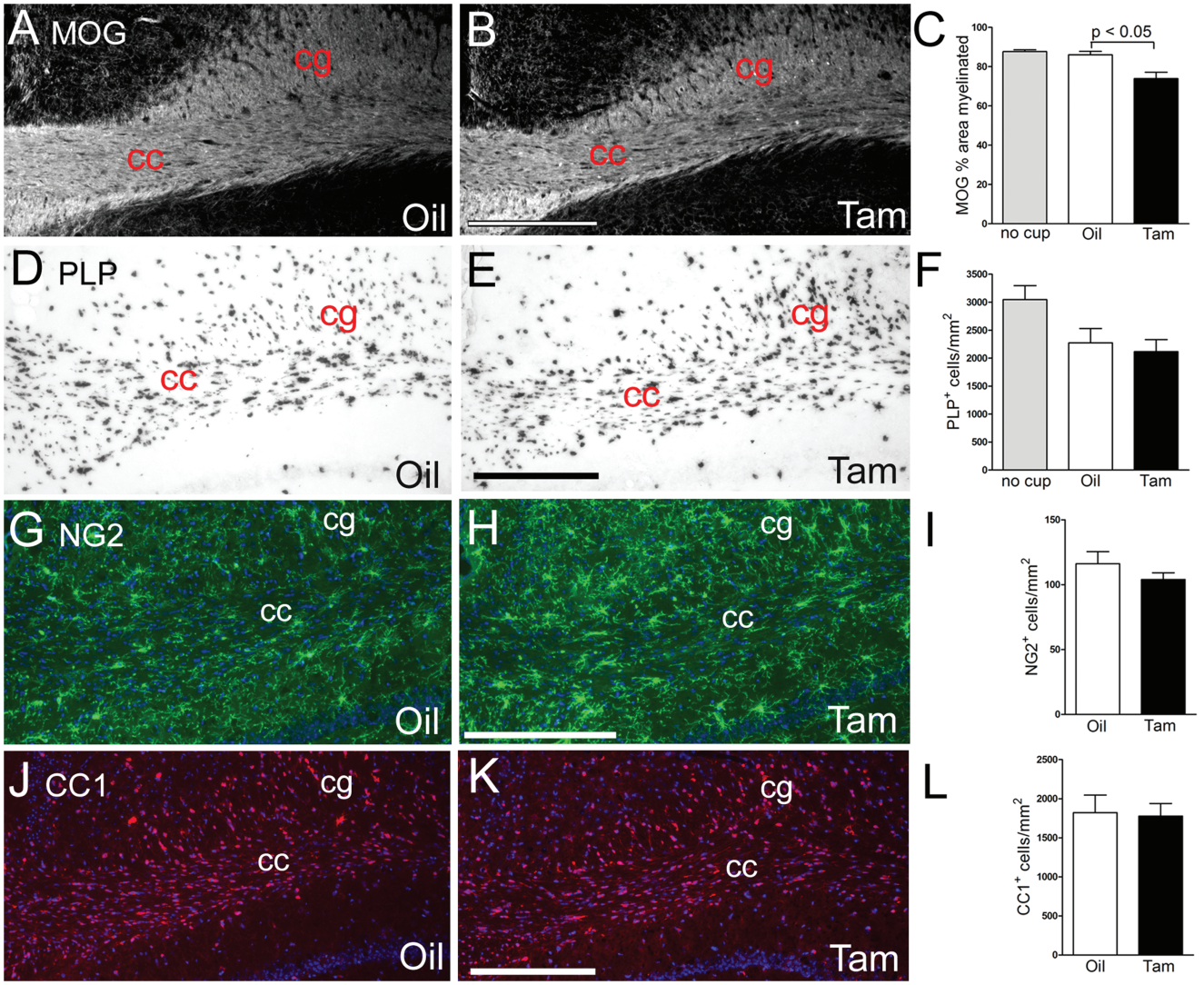

FIGURE 4 LRF knockdown impairs remyelination, but not oligodendrocyte repopulation, after demyelination from 0.2% cuprizone ingestion. Coronal sections from *Plp/CreERT:Zbtb7a*$^{fl/fl}$ mice were analyzed to determine the effect of LRF knockdown on the oligodendrocyte lineage stage and the extent of remyelination in the corpus callosum. Tamoxifen, or oil vehicle, was administered at the end of 6 weeks of 0.2% cuprizone and then mice were fed normal chow for 6 weeks to allow for spontaneous remyelination. **A-C**: Immunoreactivity for MOG shows that remyelination has progressed after 6 weeks on normal chow in mice administered oil (A) or tamoxifen (B), as compared to the demyelination observed throughout the corpus callosum at 6 weeks of 0.2% cuprizone feeding (Figure S3). In mice administered oil, the remyelination is equivalent to myelination in age-matched *Plp/CreERT:Zbtb7a*$^{fl/fl}$ mice that were not fed cuprizone (no cup; C). In mice administered tamoxifen, the remyelinated area of the corpus callosum is significantly reduced compared to the oil control mice (Cohen's *d* effect size = 2.08; C). **D-F**: PLP in situ hybridization in mice administered oil (D) or tamoxifen (E) shows similar oligodendrocyte repopulation of the corpus callosum (F), which is also similar to mice that were not fed cuprizone (no cup; F). **G-I**: Oligodendrocyte progenitors, identified by NG2 (green; G-H), in mice administered oil (G) or tamoxifen (H) were found in a similar density (I). **J-L**: Mature oligodendrocytes, identified by CC1 (red; J-K) in mice administered oil (J) or tamoxifen (K) were also present at similar levels (L). cc = corpus callosum, cg = cingulum. Scale bars = 250 um. Analysis of $n = 5$ mice per condition. ANOVA with Tukey multiple comparisons used in C, F. Student *t*-test used in I, L.

3.3 | Conditional inducible knockdown of LRF during early remyelination in *NG2CreER*^{T}*:Zbtb7a*$^{fl/fl}$ mice

To move the analysis of LRF further forward in the lineage, we performed cuprizone (0.3%) studies in *NG2CreER*^{T}*:Zbtb7a*$^{fl/fl}$ mice (Figure 6). Mice were administered tamoxifen at 4 weeks of cuprizone and then analyzed at the end of the 6 weeks of cuprizone demyelination (Figure 6a-i). Mice administered tamoxifen had significantly lower levels of corpus callosum myelin, as estimated by MOG immunoreactivity (Figure 6a-c). In mice with tamoxifen administration, the MOG area is markedly reduced (approximately 44%) and the area values are below the 97th percentile of the oil area values, based on a large Cohen's *d* effect size. After a 3-week recovery period on normal chow, myelination in mice given tamoxifen or vehicle recovered to similar levels (Figure S5). These findings indicate that LRF knockdown in *NG2CreER*^{T}*:Zbtb7a*$^{fl/fl}$ mice impaired the early remyelination that occurs as

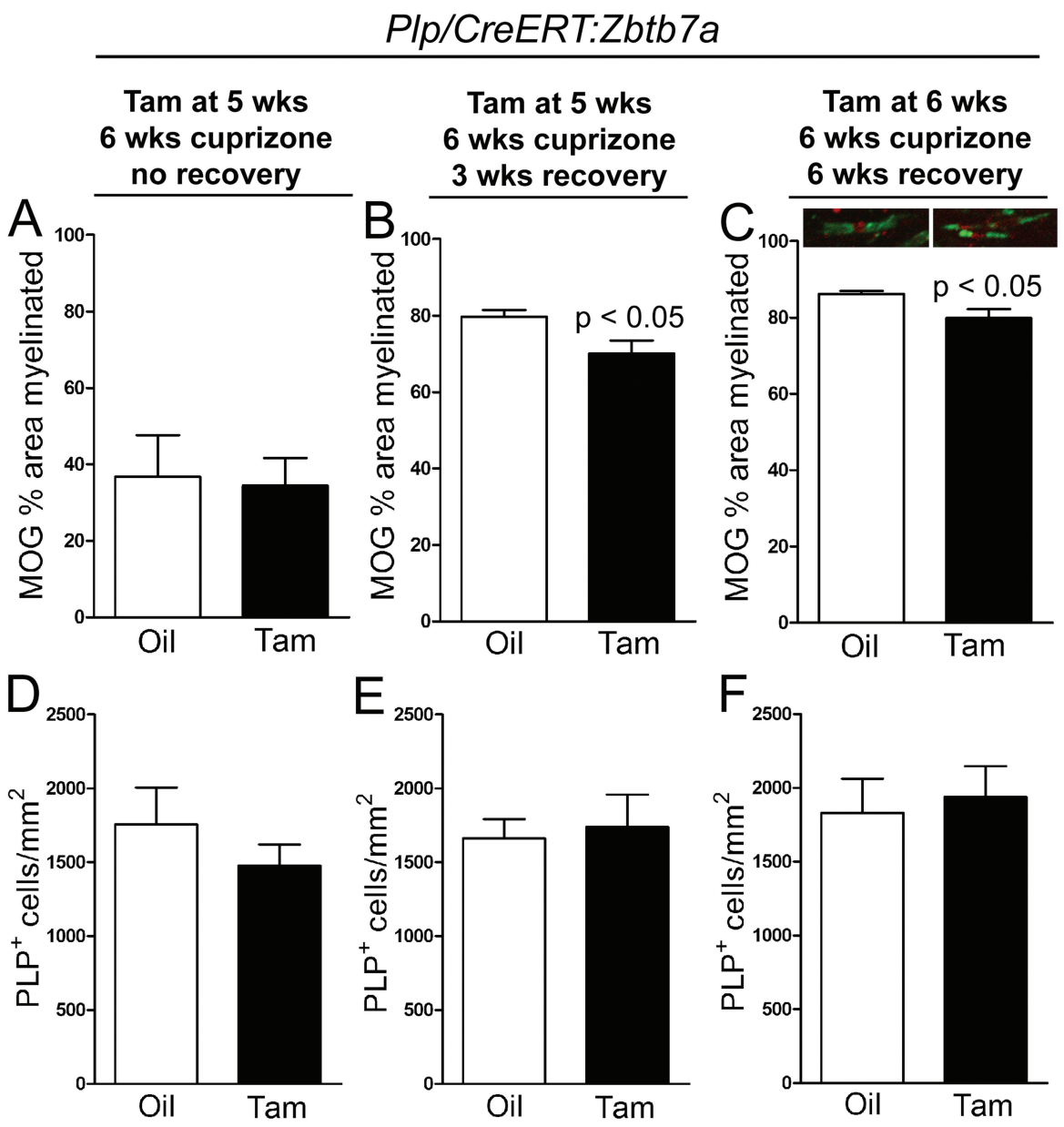

FIGURE 5 Tamoxifen administration in Plp/CreERT:Zbtb7a$^{fl/fl}$ mice impairs remyelination, but not oligodendrocyte repopulation, after demyelination from 0.3% cuprizone ingestion. Demyelination of the corpus callosum was induced in *Plp/CreERT:Zbtb7a$^{fl/fl}$* mice by feeding 0.3% cuprizone for 6 weeks. A higher dose of cuprizone was used to maximize demyelination and oligodendrocyte loss while allowing continuous access to either the training or complex wheel configuration. Mice were administered tamoxifen (Tam), or vehicle (Oil) after week 5 of cuprizone feeding and then perfused at the end of week 6 on cuprizone (no recovery; A, D) or after a 3 week period on a normal chow diet to allow for spontaneous remyelination (3 wks recovery; B, E). The mice analyzed for the 6 week recovery time point (6 wks recovery; C, F) are from the wheel assessments shown in Figure S3 and so were given tamoxifen at the end of the 6 week period of cuprizone demyelination. Quantification of MOG immunoreactivity was used to estimate the myelinated area of the corpus callosum (A-C). In mice administered tamoxifen to knockdown LRF, the extent of remyelination is significantly reduced at both the 3 and 6 week time points of the recovery period (3 weeks, $p < 0.0364$, Cohen's d effect size = 1.35, $n = 6$ oil, $n = 7$ tamoxifen; 6 weeks, $p < 0.0296$, Cohen's d effect size = 1.67, n = 5 oil, n = 5 tamoxifen). Immunolabeling for Caspr (green) and Nav1.6 (red) indicates relatively normal organization of the node of Ranvier with the progression of remyelination in mice administered oil while examples of disrupted broader nodes continued to be found in mice administered tamoxifen (C). PLP in situ hybridization shows similar oligodendrocyte repopulation of the corpus callosum in mice administered tamoxifen or oil (D-F).

oligodendrocytes are generated while mice are still on cuprizone at 6 weeks. LRF knockdown appeared to also reduce the density of oligodendrocytes, identified by PLP expression, but this effect was not statistically significant (Figure 6d-f). The density of OP cells, detected with in situ hybridization for PDGF alpha-receptor (PDGFaR), was not different in tamoxifen versus vehicle treated mice (Figure 6g-i). This result is consistent with LRF expression in only a minority of OP cells so that LRF deletion should have little effect at the OP stage.

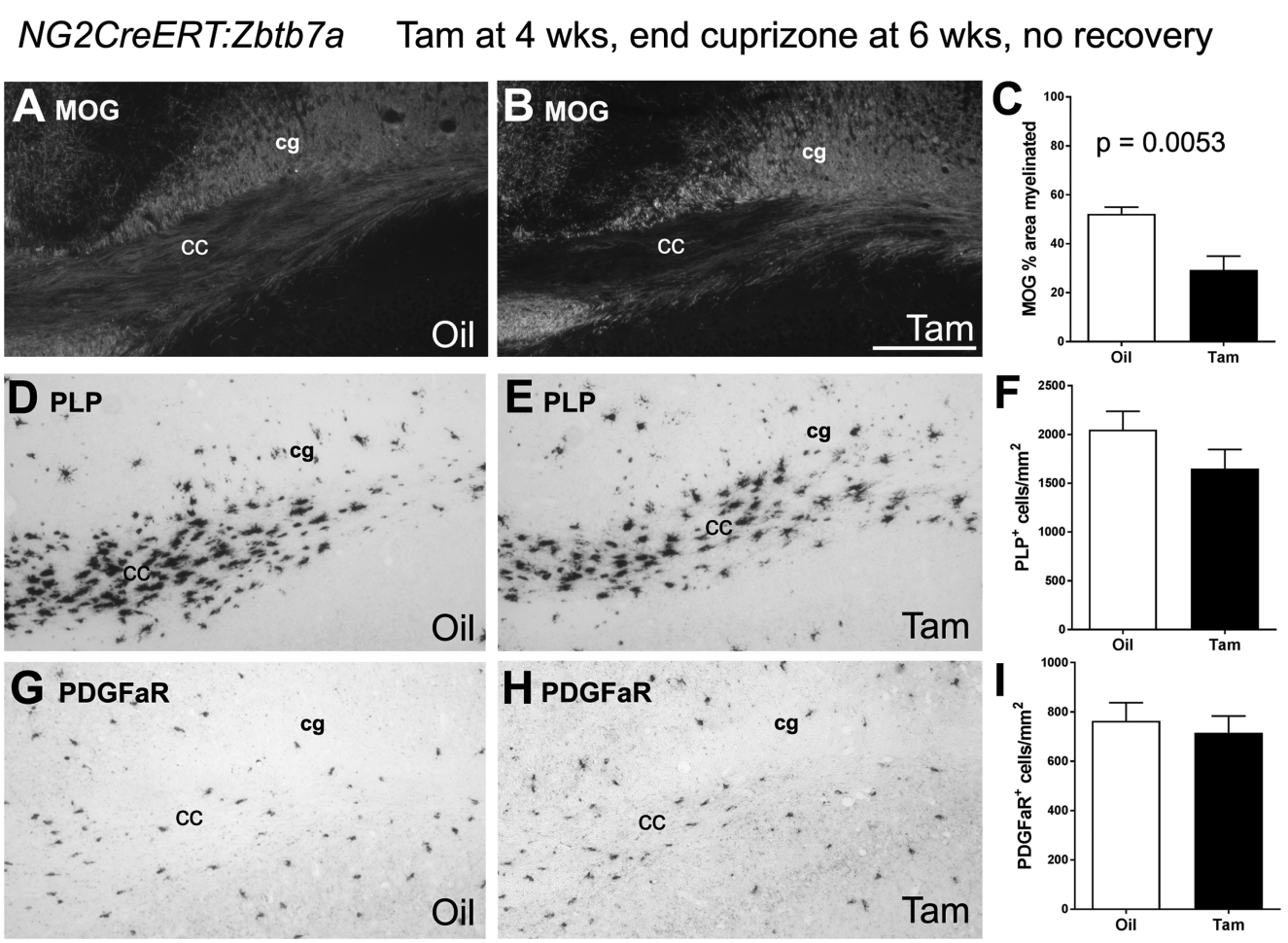

FIGURE 6 Tamoxifen administration in NG2CreERT:Zbtb7a$^{fl/fl}$ mice impairs remyelination after demyelination from 0.3% cuprizone ingestion. Demyelination of the corpus callosum was induced in *NG2CreERT:Zbtb7a$^{fl/fl}$* mice by feeding 0.3% cuprizone for 6 weeks. Mice were administered tamoxifen (Tam), or vehicle (Oil) after week 4 of cuprizone feeding and then perfused at the end of week 6 on cuprizone. Tamoxifen (Tam) administration significantly reduced the extent of remyelination determined by MOG immunoreactivity (A-C; $p = 0.0053$, Cohen's d effect size = 1.98, $n = 6$ oil, $n = 7$ tamoxifen). Tamoxifen appeared to reduce the generation of oligodendrocytes (D-F) but this difference was not statistically significant ($p = 0.1726$). Tamoxifen did not change the OP cell density (G-I). cc = corpus callosum, cg = cingulum. Scale bar in H = 100 um.

3.4 | LRF transcriptional regulation of genes for myelin biogenesis and notch target genes

To gain insight as to the potential role of LRF in acting as a transcription factor relevant to remyelination, we co-transfected OP cells with an LRF expression plasmid and myelin gene promoter element plasmids driving luciferase expression (Figure 7). This analysis included the promoters for MBP and CNP, which are repressed by Hes5 (Liu et al., 2006), since LRF has been associated with the notch-signaling pathway (Lee et al., 2013; Maeda et al., 2007). Transcriptional activity from the full length MBP promoter was highest in OP cells grown in defined medium (i.e., without mitogens), which indicates appropriate transcriptional regulation during OP differentiation (Figure 7a). LRF significantly repressed transcription from the full length MBP promoter (Figure 7a). LRF regulation of a truncated MBP promoter was then used to examine dependence on Sp1 transcription factor binding sites. LRF can interact with Sp1 promoter elements and Sp1 phosphorylation initiates upregulation of MBP (Choi et al., 2008; Guo, Eviatar-Ribak, & Miskimins, 2010). In conditions that promoted differentiation, LRF repression of the truncated MBP required an intact Sp1 site (Figure 7b,c). The second myelin-specific gene, CNP, is expressed from an early stage in the oligodendrocyte lineage (Zhang et al., 2009); accordingly, the CNP promoter response was expressed similarly with and without mitogens present. CNP transcription was strongly repressed by LRF in both growth conditions (Figure 7d). Finally, analysis was extended to the promoter for FASN, which encodes fatty acid synthase, a key enzyme in the synthesis of the fatty acid palmitate that is essential for lipids in cell membranes and myelin (Smith, Witkowski, & Joshi 2003). In contrast to MBP and CNP, FASN promoter activity was not reduced by the presence of LRF in defined medium, which promoted differentiation (Figure 7e). However, LRF significantly increased FASN promoter activity in mitogenic conditions that maintained OP cells in an immature, proliferative stage (Figure 7e). These myelin gene promoter assays indicate that LRF has the potential to regulate myelin gene transcription in a context dependent manner.

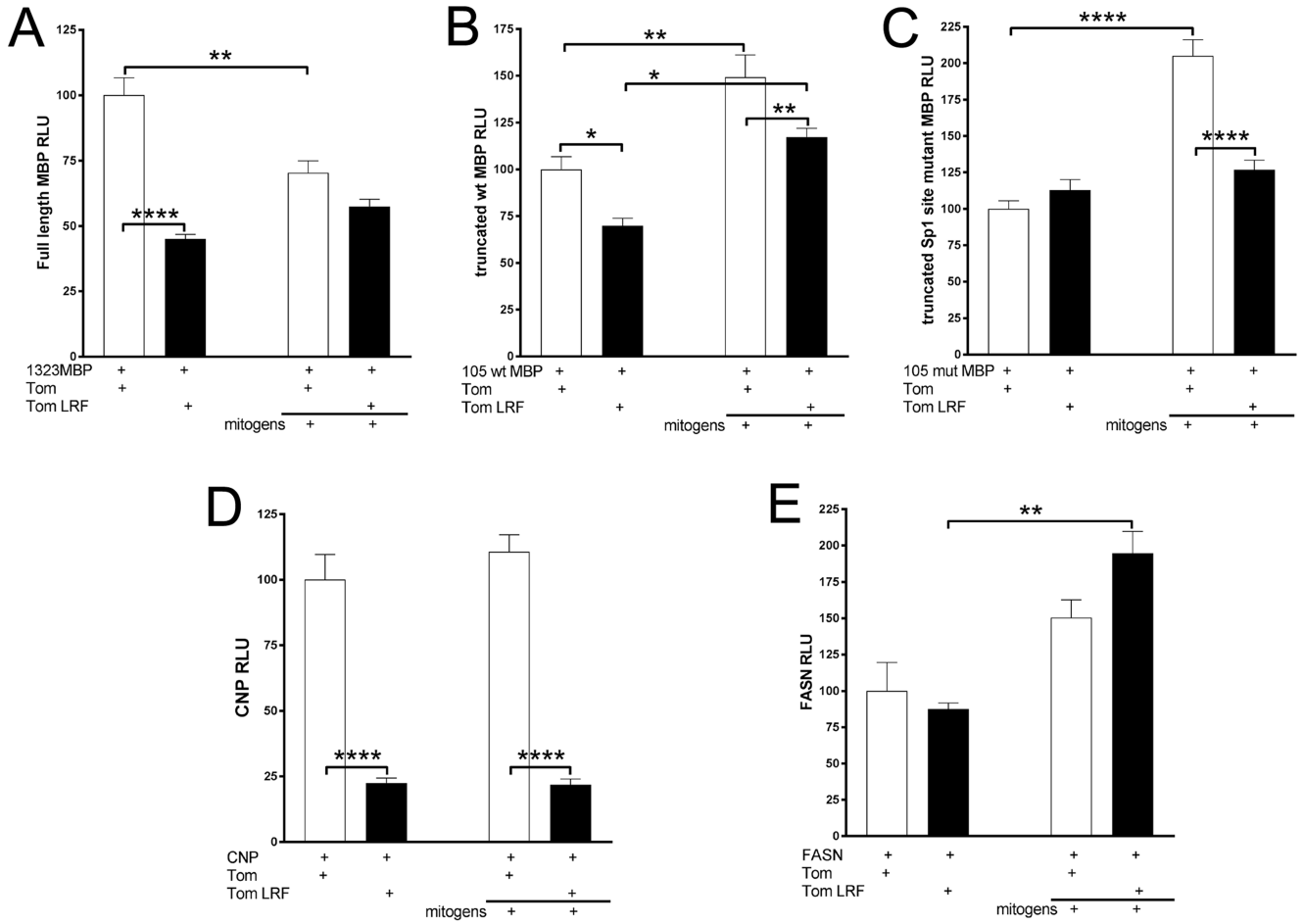

FIGURE 7 LRF transcriptional regulation of myelin genes. Transcriptional activity was measured from transient transfections of OP cultures with expression plasmids either with (Tom-LRF) or without (Tom) the *Zbtb7a* insert encoding LRF, along with firefly luciferase plasmids containing myelin promoter elements, and Renilla luciferase as an internal control. Transcription from the full-length promoter for myelin basic protein (1323MBP) is significantly higher in defined medium (**$p = 0.0017$), indicating appropriate upregulation as expected during OP differentiation in vitro (A). Co-transfection with the Tom-LRF plasmid significantly represses transcription from 1323MBP in defined medium (****$p < 0.0001$; A). Further, in defined medium, LRF repression of a truncated 105 bp MBP promoter requires the intact wild type Sp1 site (*$p = 0.0326$; B) and is not observed with the mutation to prevent Sp1 binding (C). In the presence of mitogens, LRF does not alter transcription from the full-length 1323MBP promoter (A) yet gains repressive activity using the truncated construct with the wild type sequence (**$p = 0.0032$; B) and with the Sp1 site mutated (****$p < 0.0001$; C). LRF expression significantly represses transcription from the 2',3'-cyclic-nucleotide 3'-phoshodiesterase (CNP) promoter in both growth conditions (****$p < 0.0001$; D). In the presence of LRF, transcription of fatty acid synthase from FASN is significantly increased by the addition of mitogens (**$p = 0.0037$; E). Two-way ANOVA using values combined from four independent experiments.

The role of LRF in transcriptional regulation of the notch pathway was tested using promoter constructs of notch target genes, Hes1 and Hes5 (Figure 8). In cultures of OP cells in the presence of mitogens, LRF enhanced Hes1 transcription (Figure 8a). Co-transfection with Notch1IC increases notch tone and inhibits OP differentiation (Zhou et al., 2007). In the presence of Notch1IC, LRF enhanced transcription from the Hes1 promoter, but only in the presence of mitogens (Figure 8b). LRF repressed Hes5 transcription in OP cells cultured with mitogens (Figure 8c). In the presence of Notch1IC, LRF significantly repressed Hes5 transcriptional activity both in defined medium and in the presence of mitogens (Figure 8d). Therefore, LRF specifically represses Hes5 transcription in OP cells across growth conditions (Figure 8c,d). The potential for LRF and notch pathway interactions to play a role during remyelination is indicated by Notch1 and Jagged1 upregulation in cuprizone lesions along with LRF co-localization in cells expressing Hes5 (Supplemental Figure S6). This time point of 5 weeks of cuprizone ingestion corresponds well with the 4-6 week cuprizone period of LRF knockdown that reduced MOG in *NG2CreER^T:Zbtb7a$^{fl/fl}$* mice (Figure 6a).

4 | DISCUSSION

We present the first study of LRF expression and function in CNS pathology. LRF was examined in the context of demyelination, followed by oligodendrocyte regeneration and remyelination. This work shows nuclear LRF immunoreactivity in the majority of oligodendrocytes, but only rarely in OP stage cells. Therefore, LRF function was further examined in vivo with conditionally induced knockdown of LRF in

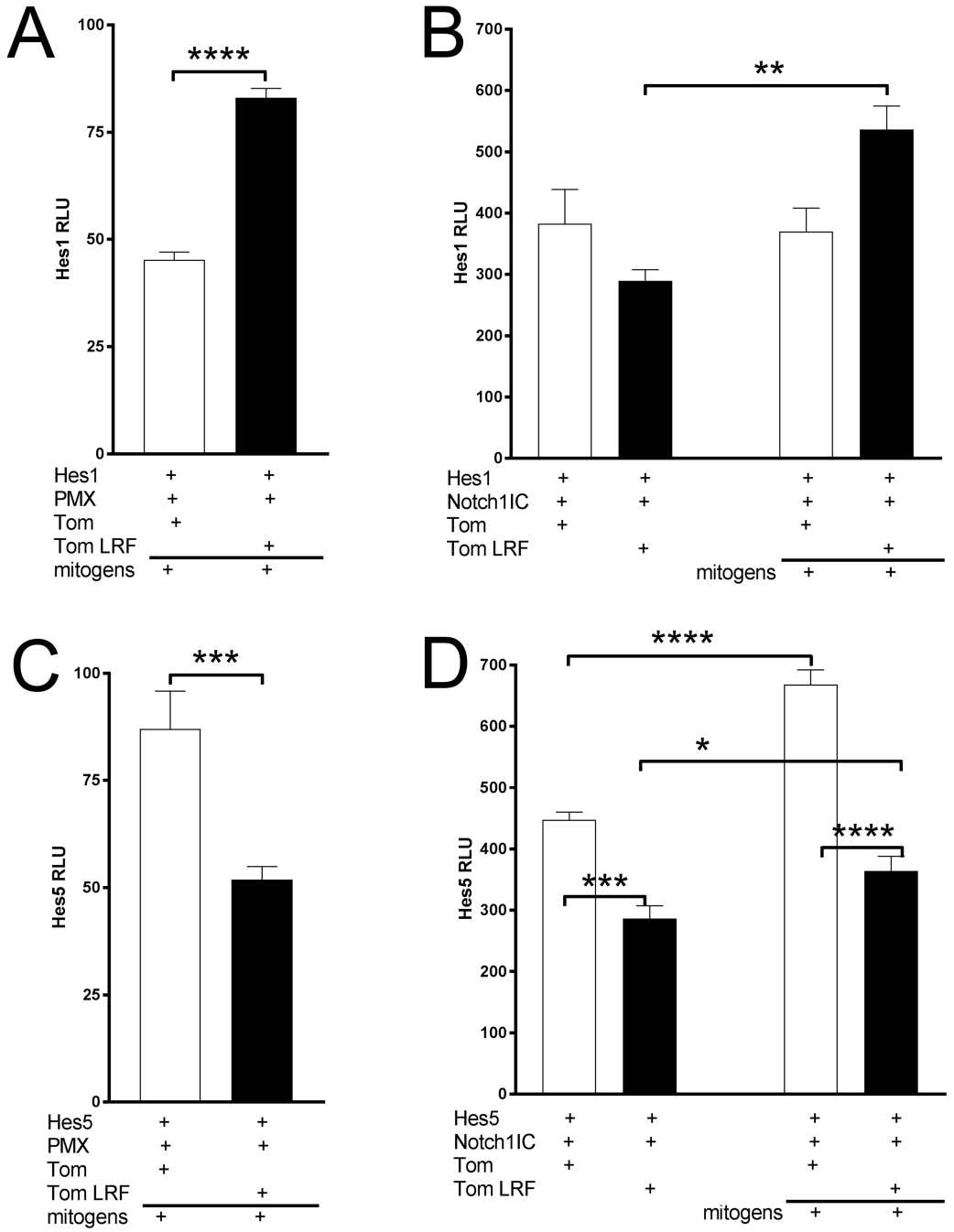

FIGURE 8 LRF transcriptional regulation of notch target genes. Transcriptional activity was measured from transient transfections of OP cultures with expression plasmids either with (+) or without (-) the *Zbtb7a* insert encoding LRF, along with firefly luciferase plasmids containing Hes1 and Hes5 promoter elements, and Renilla luciferase as an internal control. LRF enhances transcriptional activity from the Hes1 promoter, but only in the presence of mitogens (A, B). LRF represses transcription from the Hes5 promoter across all growth conditions (C, D). Notch1 intracellular domain (Notch1IC) construct was co-transfected to test the effect of LRF with increased notch tone (B, D). Transcriptional activity is shown as relative light units (RLU) normalized as firefly values divided by Renilla control readings. Values combined from four independent experiments.

oligodendrocytes after cuprizone demyelination. Oligodendrocyte repopulation of demyelinated areas in the corpus callosum did not change with LRF knockdown in *Plp/CreER^T:Zbtb7a$^{fl/fl}$* mice; however, the extent of remyelination was modestly, yet significantly, reduced at both 3-and 6-week time points of recovery on normal chow. Conditionally induced deletion of LRF earlier in the oligodendrocyte lineage in *NG2CrER^T:Zbtb7a$^{fl/fl}$* mice showed earlier and more marked reduction of myelination after 6 weeks of cuprizone demyelination. In vitro transcription assays in OP cells unexpectedly showed LRF repression of myelin genes, yet enhanced transcription of FASN in the presence of mitogens. Further in vitro transcription assays showed LRF repression of Hes5, indicating a potential role in notch signaling in OP cells.

4.1 | LRF regulation of transcriptional activity in OP cell cultures

A potential role for LRF in exerting transcriptional control in oligodendrocyte lineage cells is demonstrated through our in vitro promoter assay data (Figures 7, 8). The identified promoter consensus sequence for LRF binding is a GC-rich sequence ([G/A][C/A]GACCCC), with the underlined cytosines being essential core nucleotides (Lunardi et al., 2013; Maeda et al., 2005; Wang et al., 2012). Within the promoter elements tested, those that showed repression contain one or more potential LRF consensus sites in the proximal promoter region. However, LRF binding of DNA appears flexible and may involve a single site or two half sites with variable orientation and separation (Lee et al., 2013; Pessler & Hernandez, 2003). Therefore, direct DNA binding of LRF cannot be predicted solely from a given promoter sequence.

Myelin-specific genes are regulated by epigenetic marks and a hierarchy of transcription factors that vary with lineage stage (Fulton, Denarier, Friedman, Wasserman, & Peterson, 2011; Hernandez & Casaccia, 2015). The epigenetic landscape of myelin-specific promoters may be particularly important for LRF binding or the effect of LRF molecular interactions, such as recruitment of HDACs (Liu et al., 2004), which must occur at the appropriate time and site. Our experiments of LRF expression from transfection in OP cells may provide insights from the context-dependent effect elicited by the testing in two growth conditions (Figure 7). Growth in defined medium initiates OP differentiation and increased transcription from the full length MBP promoter (Figure 7). Similar studies have shown that protein kinase C phosphorylates Sp1 to increase MBP transcription in differentiated oligodendrocytes, but not in proliferating OP cells (Guo et al., 2010). LRF may repress MBP transcription in differentiating oligodendrocytes through interaction with phosphorylated Sp1 binding, which is abolished by mutation of the Sp1 site (Figure 7a-c). This effect is similar to that seen on the Rb tumor suppressor gene in cancer cells, where LRF can repress transcription through interaction with Sp1 and recruitment of histone deacetylase (Jeon et al., 2008).

Sp1 may also be involved in LRF regulation of FASN in oligodendrocyte lineage cells. LRF interacts with SREBP-1 at Sp1 sites to synergistically activate FASN transcription in multiple cell lines (Choi et al., 2008). FASN is a key enzyme in fatty acid synthesis that is essential for phospholipids in myelin and cell membranes (Smith et al., 2003). In OP cells, SREBPs are important regulators of oligodendrocyte maturation and FASN levels (Monnerie et al., 2017). A high demand for lipids is associated with membrane biogenesis for cell division and for formation of myelin. The short term culture conditions used for promoter analysis during OP differentiation were not sufficient to test the role of LRF on FASN transcription during myelin sheath elaboration. In the presence of mitogens that stimulate OP proliferation, LRF co-transfection resulted in transcriptional activation of the FASN promoter (Figure 7e). A positive effect of LRF on FASN levels in conditions of high membrane biogenesis would be consistent with continued expression of LRF in mature oligodendrocytes (Figure 2). This role for LRF would also be consistent with the reduced remyelination after LRF knockdown (Figures 4–6).

CNP, another myelin-specific gene, was strongly repressed by LRF, regardless of growth condition (Figure 7d) and is not known to be regulated by Sp1 phosphorylation (Fulton et al., 2011). MBP and CNP have been shown to be repressed by Hes5 (Liu et al., 2006). Therefore, LRF overexpression could be expected to release or de-repress MBP and CNP from Hes5 repression. Importantly, in vitro LRF co-transfection reduced MBP and CNP promoter activity (Figure 7), which is not consistent with our in vivo results of reduced myelin levels with LRF knockdown during remyelination (Figures 4–6). A potential explanation for this in vitro result is that LRF is overexpressed after transfection of the LRF plasmid. A further explanation may be that transfection at the OP cell stage is ectopic since LRF is not expressed in the majority OP cells in vivo. Furthermore, the binding sites of transfected MBP and CNP promoter constructs may not undergo the epigenetic modifications in myelin genes that occur with lineage progression. This artificial approach thus reveals a potent LRF repression of these myelin gene promoters, especially CNP, early in the lineage that must undergo as yet unknown modifications to prevent this potent repression of myelin genes in mature oligodendrocytes. Since high levels of membrane biogenesis are required for both cell proliferation and myelin formation, FASN may not be as restricted to such cell stage specific promoter modifications. Along these lines, we note that the adult brain and spinal cord exhibits strong LRF expression in neurons, which also have a high level of membrane biogenesis to maintain extensive processes and continuously synthesize vesicles for axonal transport.

4.2 | The lesion context of remyelination in MHV and cuprizone models

Two distinct models of experimental demyelination were used to exploit the advantages of each in our studies of LRF. The MHV model produces multiple sclerosis-like lesions with environmental signals associated with lytic infection of oligodendrocytes, microglial activation, astrogliosis, and lymphocytic infiltration (Armstrong et al., 2005). After viral clearance mediated through a Th1 immune response, demyelinated areas undergo effective spontaneous remyelination (Jordan et al., 1989; Parra et al., 1999). MHV lesions have increased expression of diverse cytokines and mitogens, including PDGF and FGF2 mitogens (Messersmith et al., 2000; Redwine & Armstrong, 1998). Therefore, characterization of LRF in MHV lesions provides a context of pathological features shared with multiple sclerosis lesions and mitogen signaling relevant to our in vitro promoter assays.

For several reasons related to the handling of virus infected mice and the high number of mice needed per experiment, the MHV model is not optimal for in vivo knockdown to test LRF function during remyelination. A proportion of virus infected mice die while others remain asymptomatic (Armstrong et al., 2005). In addition, tamoxifen may alter disease progression in female mice through binding of endogenous estrogen receptors, which raises concern for using female mice in studies utilizing tamoxifen-induced recombination (Klinge, Studinski-Jones, Kulakosky, Bambara, & Hilf, 1998). Indeed, the severity of demyelination varies with estrus stage in female mice while male mice

undergo progressive disease with high mortality (Armstrong et al., 2005).

We have used the cuprizone model effectively with tamoxifen administration to reveal effects of gene deletion during remyelination (Mierzwa et al., 2013; Zhou et al., 2012). The cuprizone model produces extensive demyelination of the corpus callosum that involves a well-documented progression of OP proliferation and differentiation leading to efficient spontaneous remyelination (Hibbits, Yoshino, Le, & Armstrong, 2012; Matsushima & Morell, 2001). Cuprizone ingestion results in high OP proliferation after 4-5 weeks and is followed by initial oligodendrocyte repopulation of lesions within 6 weeks (Armstrong et al., 2006; Armstrong et al., 2002). Cuprizone demyelinated lesions include several factors examined in our in vitro promoter assays. Namely, cuprizone lesions exhibit upregulation of the mitogens PDGF and FGF2 (Armstrong et al., 2006; Armstrong et al., 2002; Vana, Lucchinetti, Le, & Armstrong, 2007a). Notch1 is also upregulated in proliferating OP cells and Jagged1 is present in lesion areas (Figure S6). Furthermore, Hes5 is present in OP cells and HDAC1 binding to the Hes5 promoter is increased during cuprizone demyelination, followed by normalization early in remyelination (Shen et al., 2008). Hes5 inhibits OP differentiation into mature oligodendrocytes in the context of both developmental myelination and remyelination (Kondo & Raff, 2000; Liu et al., 2006; Shen et al., 2008; Wang et al., 1998). Hes5 may also be a downstream partner that intersects with fibroblast growth factor signaling, which inhibits OP differentiation in demyelinated lesions (Zhou & Armstrong, 2007).

4.3 | LRF in the context of remyelination

LRF function was tested in the corpus callosum using conditional deletion induced in oligodendrocyte lineage cells prior to remyelinaton in *Plp/CreER^T:Zbtb7a$^{fl/fl}$* mice. During remyelination, LRF was expressed in 94% of Olig2 cells; the LRF negative subset presumably overlapped with the NG2 + OP population that comprised 5% of Olig2 cells (Figures 3, 4). Tamoxifen administration in *Plp/CreER^T:Zbtb7a$^{fl/fl}$* mice knocked down LRF expression to 41% among Olig2 cells. LRF deletion in Olig2 cells did not reduce the total oligodendrocyte lineage population (Figure 3). Somewhat surprisingly, LRF knockdown also did not alter the proportion of mature oligodendrocytes versus OP cells, with NG2 + OP cells comprising 3% of the Olig2 population in mice administered tamoxifen (Figure 4). This finding is in contrast to our study of postnatal myelination during spinal cord development in which LRF knockdown inhibited differentiation to increase OP cells at the expense of oligodendrocytes (Dobson et al., 2012).

LRF knockdown significantly reduced the extent of remyelination in three independent cohorts of *Plp/CreER^T:Zbtb7a$^{fl/fl}$* mice, with no significant change in oligodendrocyte repopulation (Figures 4, 5). The deficit of remyelination was not sufficient to impair running on complex wheels (Figure S4). Impairment on the complex wheel assessment has corresponded well with MOG detection of myelination status in the corpus callosum in our prior cuprizone studies (Hibbits et al., 2009; Mierzwa et al., 2013). Additional assessments may be needed to detect more subtle effects from reduced remyelination, including changing the conditions of the complex wheel assessment to test motor skill learning (McKenzie et al., 2014).

LRF knockdown in *NG2CrER^T:Zbtb7a$^{fl/fl}$* mice earlier in the oligodendrocyte lineage resulted in more dramatic reduction in myelination after 6 weeks of cuprizone (Figure 6). However, during the recovery period after demyelination, the extent of remyelination remained reduced with tamoxifen administration in *Plp/CreER^T:Zbtb7a$^{fl/fl}$* mice (Figures 4–5) but recovered to vehicle levels in *NG2CrER^T:Zbtb7a$^{fl/fl}$* mice (Figure S5). Together, these results indicate that LRF acts at a late OP and/or mature oligodendrocyte stage to modulate the extent of remyelination.

5 | CONCLUSION

LRF is strongly expressed in the adult CNS. In the oligodendrocyte lineage, LRF is expressed in only a small proportion of OP cells while it is present in nuclei of the majority of oligodendrocytes. LRF is not required for oligodendrogenesis, possibly because of the late expression of LRF in the lineage. LRF modulates the extent of remyelination, indicating potential regulation of myelin synthesis after the generation of oligodendrocytes. Further elucidating the role of LRF may require knockdown and overexpression of highly related proteins to reveal redundancy. For example, deletion of LRF or ThPOK singly does not alter T-cell expression of CD4 or functional differentiation yet disruption of both proteins shows redundant roles in maintaining the CD4 lineage (Vacchio et al., 2014).

ACKNOWLEDGMENTS

This work was supported by the National Multiple Sclerosis Society, grant numbers: RG 4224; RG 4675. NK performed the work as a Prince Mahidol Scholar with support from the government of Thailand. We thank those who provided plasmids and mouse lines, as noted in the text. We also thank Xiaomei Zi for technical assistance. Associate Editor: Ernesto Bongarzone

CONFLICT OF INTEREST STATEMENT

No conflicting interests exist.

ROLE OF AUTHORS

All authors had full access to all the data in the study and take responsibility for the integrity of the data and the accuracy of the data analysis. Study concept and design: RCA, NLD. Acquisition of data: NLD, FY, NK, TQL, LAB, KLR, RCA. Analysis and interpretation of data: NLD, FY, NK, KLR, RCA. Critical revision of the manuscript for important intellectual content: NLD, FY, NK, RCA. Statistical analysis: NLD, FY, NK, RCA. Obtained funding: NK, RCA. Study supervision: RCA.

DECLARATION OF TRANSPARENCEY

The authors, reviewers and editors affirm that in accordance to the policies set by the Journal of Neuroscience Research, this manuscript

presents an accurate and transparent account of the study being reported and that all critical details describing the methods and results are present.

REFERENCES

Armstrong, R.C. (1998). Isolation and characterization of immature oligodendrocyte lineage cells. *Methods*, *16*, 282-292.

Armstrong, R.C., Kim, J.G., & Hudson, L.D. (1995). Expression of myelin transcription factor I (MyTI), a "zinc-finger" DNA-binding protein, in developing oligodendrocytes. *Glia*, *14*, 303-321.

Armstrong, R.C., Le, T.Q., Flint, N.C., Vana, A.C., & Zhou, Y.X. (2006). Endogenous cell repair of chronic demyelination. *Journal of Neuropathology and Experimental Neurology*, *65*, 245-256.

Armstrong, R.C., Le, T.Q., Frost, E.E., Borke, R.C., & Vana, A.C. (2002). Absence of fibroblast growth factor 2 promotes oligodendroglial repopulation of demyelinated white matter. *The Journal of Neuroscience*, *22*, 8574-8585.

Armstrong, R.C., Redwine, J.M., Messersmith, D.J. (2005). Coronavirus-induced demyelination and spontaneous remyelination: growth factor expression and function. In: E. Lavi, & C.S. Constantinescu (Eds.). *Experimental models of multiple sclerosis*. Norwell, MA: Kluver.

Breithaupt, C., Schubart, A., Zander, H., Skerra, A., Huber, R., Linington, C., & Jacob, U. (2003). Structural insights into the antigenicity of myelin oligodendrocyte glycoprotein. *Proceedings of the National Academy of Sciences of the United States of America*, *100*, 9446-9451.

Choi, W.I., Jeon, B.N., Park, H., Yoo, J.Y., Kim, Y.S., Koh, D.I., … Hur, M. W. (2008). Proto-oncogene FBI-1 (Pokemon) and SREBP-1 synergistically activate transcription of fatty-acid synthase gene (FASN). *Journal of Biological Chemistry*, *283*, 29341-29354.

Dobson, N.R., Moore, R.T., Tobin, J.E., & Armstrong, R.C. (2012). Leukemia/lymphoma-related factor regulates oligodendrocyte lineage cell differentiation in developing white matter. *Glia*, *60*, 1378-1390.

Doerflinger, N.H., Macklin, W.B., & Popko, B. (2003). Inducible site-specific recombination in myelinating cells. *Genesis*, *35*, 63-72.

Fulton, D.L., Denarier, E., Friedman, H.C., Wasserman, W.W., & Peterson, A.C. (2011). Towards resolving the transcription factor network controlling myelin gene expression. *Nucleic Acids Research*, *39*, 7974-7991.

Gallo, V., & Deneen, B. (2014). Glial development: the crossroads of regeneration and repair in the CNS. *Neuron*, *83*, 283-308.

Goretzki, L., Burg, M.A., Grako, K.A., & Stallcup, W.B. (1999). High-affinity binding of basic fibroblast growth factor and platelet-derived growth factor-AA to the core protein of the NG2 proteoglycan. *The Journal of Biological Chemistry*, *274*, 16831-16837.

Guo, L., Eviatar-Ribak, T., & Miskimins, R. (2010). Sp1 phosphorylation is involved in myelin basic protein gene transcription. *Journal of Neuroscience Research*, *88*, 3233-3242.

Hammond, T.R., Gadea, A., Dupree, J., Kerninon, C., Nait-Oumesmar, B., Aguirre, A., & Gallo, V. (2014). Astrocyte-derived endothelin-1 inhibits remyelination through notch activation. *Neuron*, *81*, 588-602.

He, Y., Sandoval, J., & Casaccia-Bonnefil, P. (2007). Events at the transition between cell cycle exit and oligodendrocyte progenitor differentiation: the role of HDAC and YY1. *Neuron Glia Biology*, *3*, 221-231.

Hernandez, M., & Casaccia, P. (2015). Interplay between transcriptional control and chromatin regulation in the oligodendrocyte lineage. *Glia*, *63*, 1357-1375.

Hibbits, N., Pannu, R., Wu. T.J., & Armstrong, R.C. (2009). Cuprizone demyelination of the corpus callosum in mice correlates with altered social interaction and impaired bilateral sensorimotor coordination. *ASN Neuro*, *1*(3) e00013: doi:10.1042/AN20090032.

Hibbits, N., Yoshino, J., Le, T.Q., & Armstrong, R.C. (2012). Astrogliosis during acute and chronic cuprizone demyelination and implications for remyelination. *ASN Neuro*, *4*, 393-408.

Jeon, B.N., Yoo, J.Y., Choi, W.I., Lee, C.E., Yoon, H.G., & Hur, M.W. (2008). Proto-oncogene FBI-1 (Pokemon/ZBTB7A) represses transcription of the tumor suppressor Rb gene via binding competition with Sp1 and recruitment of co-repressors. *Journal of Biological Chemistry*, *283*, 33199-33210.

John, G.R., Shankar, S.L., Shafit-Zagardo, B., Massimi, A., Lee, S.C., Raine, C.S., & Brosnan C.F. (2002). Multiple sclerosis: re-expression of a developmental pathway that restricts oligodendrocyte maturation. *Nature Medicine*, *8*, 1115-1121.

Jones, L.L., Yamaguchi, Y., Stallcup, W.B., & Tuszynski, M.H. (2002). NG2 is a major chondroitin sulfate proteoglycan produced after spinal cord injury and is expressed by macrophages and oligodendrocyte progenitors. *The Journal of Neuroscience*, *22*, 2792-2803.

Jordan, C.A., Friedrich, V.L. Jr., Godfraind, C., Cardellechio, C.B., Holmes, K.V., & Dubois-Dalcq, M. (1989). Expression of viral and myelin gene transcripts in a murine CNS demyelinating disease caused by a coronavirus. *Glia*, *2*, 318-329.

Klinge, C.M., Studinski-Jones, A.L., Kulakosky, P.C., Bambara, R.A., & Hilf, R. (1998). Comparison of tamoxifen ligands on estrogen receptor interaction with estrogen response elements. *Molecular and Cellular Endocrinology*, *143*, 79-90.

Kondo, T., & Raff, M. (2000). Basic helix-loop-helix proteins and the timing of oligodendrocyte differentiation. *Development*, *127*, 2989-2998.

Kopan, R., & Weintraub, H. (1993). Mouse notch: expression in hair follicles correlates with cell fate determination. *Journal of Cell Biology*, *121*, 631-641.

Kremer, D., Kury, P., & Dutta, R. (2015). Promoting remyelination in multiple sclerosis: current drugs and future prospects. *Multiple Sclerosis Journal*, *21*, 541-549.

Lee, S.U., Maeda, M., Ishikawa, Y., Li, S.M., Wilson, A., Jubb, A.M., … Maeda, T. (2013). LRF-mediated Dll4 repression in erythroblasts is necessary for hematopoietic stem cell maintenance. *Blood*, *121*, 918-929.

Lee, S.U., & Maeda, T. (2012). POK/ZBTB proteins: an emerging family of proteins that regulate lymphoid development and function. *Immunological Reviews*, *247*, 107-119.

Linnington, C., Webb, M., & Woodhams, P.L. (1984). A novel myelin-associated glycoprotein defined by a mouse monoclonal antibody. *Journal of Neuroimmunology*, *6*, 387-396.

Liu, A., Li, J., Marin-Husstege, M., Kageyama, R., Fan, Y., Gelinas, C., & Casaccia-Bonnefil, P. (2006). A molecular insight of Hes5-dependent inhibition of myelin gene expression: old partners and new players. *The EMBO Journal*, *25*, 4833-4842.

Liu, C.J., Prazak, L., Fajardo, M., Yu, S., Tyagi, N., & Di Cesare, P.E. (2004). Leukemia/lymphoma-related factor, a POZ domain-containing transcriptional repressor, interacts with histone deacetylase-1 and inhibits cartilage oligomeric matrix protein gene expression and chondrogenesis. *Journal of Biological Chemistry*, *279*, 47081-47091.

Liu, J., & Casaccia, P. (2010). Epigenetic regulation of oligodendrocyte identity. *Trends in Neuroscience*, *33*, 193-201.

Lunardi, A., Guarnerio, J., Wang, G., Maeda, T., & Pandolfi, P.P. (2013). Role of LRF/Pokemon in lineage fate decisions. *Blood*, *121*, 2845-2853.

Maeda, T., Hobbs, R.M., Merghoub, T., Guernah, I., Zelent, A., Cordon-Cardo, C., Teruya-Feldstein, J., & Pandolfi, P.P. (2005). Role of the proto-oncogene Pokemon in cellular transformation and ARF repression. *Nature*, *433*, 278-285.

Maeda, T., Merghoub, T., Hobbs, R.M., Dong, L., Maeda, M., Zakrzewski, J., ... Pandolfi PP. (2007). Regulation of B versus T lymphoid lineage fate decision by the proto-oncogene LRF. *Science*, *316*, 860-866.

Masuda, T., Wang, X., Maeda, M., Canver, M.C., Sher, F., Funnell, A.P., ... Maeda, T. (2016). Transcription factors LRF and BCL11A independently repress expression of fetal hemoglobin. *Science*, *351*, 285-289.

Matsushima, G.K., & Morell, P. (2001). The neurotoxicant, cuprizone, as a model to study demyelination and remyelination in the central nervous system. *Brain Pathology*, *11*, 107-116.

McKenzie, I.A., Ohayon, D., Li, H., de Faria, J.P., Emery, B., Tohyama, K., & Richardson, W.D. (2014). Motor skill learning requires active central myelination. *Science*, *346*, 318-322.

Messersmith, D.J., Murtie, J.C., Le, T.Q., Frost, E.E., & Armstrong, R.C. (2000). Fibroblast growth factor 2 (FGF2) and FGF receptor expression in an experimental demyelinating disease with extensive remyelination. *Journal of Neuroscience Research*, *62*, 241-256.

Mierzwa, A.J., Zhou, Y.X., Hibbits, N., Vana, A.C., & Armstrong, R.C. (2013). FGF2 and FGFR1 signaling regulate functional recovery following cuprizone demyelination. *Neuroscience Letters*, *548*, 280-285.

Monnerie, H., Romer, M., Jensen, B.K., Millar, J.S., Jordan-Sciutto, K.L., Kim, S.F., & Grinspan, J.B. (2017). Reduced sterol regulatory element-binding protein (SREBP) processing through site-1 protease (S1P) inhibition alters oligodendrocyte differentiation in vitro. *Journal of Neurochemistry*, *140*, 53-67.

Nielsen, J.A., Berndt, J.A., Hudson, L.D., & Armstrong, R.C. (2004). Myelin transcription factor 1 (Myt1) modulates the proliferation and differentiation of oligodendrocyte lineage cells. *Molecular and Cellular Neurosciences*, *25*, 111-123.

Nye, J.S., Kopan, R., & Axel, R. (1994). An activated Notch suppresses neurogenesis and myogenesis but not gliogenesis in mammalian cells. *Development*, *120*, 2421-2430.

Ohtsuka, T., Ishibashi, M., Gradwohl, G., Nakanishi, S., Guillemot, F., & Kageyama R. (1999). Hes1 and Hes5 as notch effectors in mammalian neuronal differentiation. *The EMBO Journal*, *18*, 2196-2207.

Parra, B., Hinton, D.R., Marten, N.W., Bergmann, C.C., Lin, M.T, Yang, C. S., & Stohlman, S.A. (1999). IFN-gamma is required for viral clearance from central nervous system oligodendroglia. *The Journal of Immunology*, *162*, 1641-1647.

Pessler, F., & Hernandez, N. (2003). Flexible DNA binding of the BTB/POZ-domain protein FBI-1. *Journal of Biological Chemistry*, *278*, 29327-29335.

Redwine, J.M., & Armstrong, R.C. (1998). In vivo proliferation of oligodendrocyte progenitors expressing PDGFalphaR during early remyelination. *Journal of Neurobiology*, *37*, 413-428.

Romm, E., Nielsen, J.A., Kim, J.G., & Hudson, L.D. (2005). Myt1 family recruits histone deacetylase to regulate neural transcription. *Journal of Neurochemistry*, *93*, 1444-1453.

Shen, S., Sandoval, J., Swiss, V.A., Li, J., Dupree, J., Franklin, R.J., & Casaccia-Bonnefil, P. (2008). Age-dependent epigenetic control of differentiation inhibitors is critical for remyelination efficiency. *Nature Neuroscience*, *11*, 1024-1034.

Smith, S., Witkowski, A., & Joshi, A.K. (2003). Structural and functional organization of the animal fatty acid synthase. *Progress in Lipid Research*, *42*, 289-317.

Taylor, L.C., Gilmore, W., Ting, J.P., & Matsushima, G.K. (2010). Cuprizone induces similar demyelination in male and female C57BL/6 mice and results in disruption of the estrous cycle. *Journal of Neuroscience Research*, *88*, 391-402.

Tsuji-Takechi, K., Negishi-Koga, T., Sumiya, E., Kukita, A., Kato, S., Maeda, T., ... Takayanagi H. 2012. Stage-specific functions of leukemia/lymphoma-related factor (LRF) in the transcriptional control of osteoclast development. *Proceedings of the National Academy of Sciences of the United States of America*, *109*, 2561-2566.

Vacchio, M.S., Wang, L., Bouladoux, N., Carpenter, A.C., Xiong Y, Williams LC, ... Bosselut R. (2014). A ThPOK-LRF transcriptional node maintains the integrity and effector potential of post-thymic CD4 + T cells. *Nature Immunology*, *15*, 947-956.

Vana, A.C., Flint, N.C., Harwood, N.E., Le, T.Q., Fruttiger, M., & Armstrong, R.C. (2007a). Platelet-derived growth factor promotes repair of chronically demyelinated white matter. *Journal of Neuropathology and Experimental Neurology*, *66*, 975-988.

Vana, A.C., Lucchinetti, C.F., Le, T.Q., & Armstrong, R.C. (2007b). Myelin transcription factor 1 (Myt1) expression in demyelinated lesions of rodent and human CNS. *Glia*, *55*, 687-697.

Wang, J., Zhuang, J., Iyer, S., Lin, X., Whitfield, T.W., Greven, M.C., ... Weng Z. (2012). Sequence features and chromatin structure around the genomic regions bound by 119 human transcription factors. *Genome Research*, *22*, 1798-1812.

Wang, S., Sdrulla, A.D., diSibio, G., Bush, G., Nofziger, D., Hicks, C., Weinmaster, G., & Barres, B.A. (1998). Notch receptor activation inhibits oligodendrocyte differentiation. *Neuron*, *21*, 63-75.

Wei, Q., Miskimins, W.K., & Miskimins, R. (2003). The Sp1 family of transcription factors is involved in p27(Kip1)-mediated activation of myelin basic protein gene expression. *Molecular and Cellular Biology*, *23*, 4035-4045.

Wu, Y., Liu, Y., Levine, E.M., & Rao, M.S. (2003). Hes1 but not Hes5 regulates an astrocyte versus oligodendrocyte fate choice in glial restricted precursors. *Developmental Dynamics*, *226*, 675-689.

Zhang, Y., Argaw, A.T., Gurfein, B.T., Zameer, A., Snyder, B.J., Ge, C., ... John, G.R. (2009). Notch1 signaling plays a role in regulating precursor differentiation during CNS remyelination. *Proceedings of the National Academy of Sciences of the United States of America*, *106*, 19162-19167.

Zhou, Y.X., & Armstrong, R.C. (2007). Interaction of fibroblast growth factor 2 (FGF2) and notch signaling components in inhibition of oligodendrocyte progenitor (OP) differentiation. *Neuroscience Letters*, *421*, 27-32.

Zhou, Y.X., Pannu, R., Le, T.Q., & Armstrong, R.C. (2012). Fibroblast growth factor 1 (FGFR1) modulation regulates repair capacity of oligodendrocyte progenitor cells following chronic demyelination. *Neurobiology of Disease*, *45*, 196-205.

Zhu, X., Hill, R.A., Dietrich, D., Komitova, M., Suzuki, R., & Nishiyama, A. (2011). Age-dependent fate and lineage restriction of single NG2 cells. *Development*, *138*, 745-753.

How to cite this article: Davidson NL, Yu F, Kijpaisalratana N, et al. Leukemia/lymphoma-related factor (LRF) exhibits stage- and context-dependent transcriptional controls in the oligodendrocyte lineage and modulates remyelination. *J Neuro Res*. 2017;95:2391–2408. https://doi.org/10.1002/jnr.24083